Supplementary Information

Introduction of substituents for tuning the redox properties of benzoate-bridged paddlewheel diruthenium(II, II) complexes: What does the OH group bring?

Wataru Kosaka,[a,b] Yudai Watanabe,[b] Taku Kitayama,[b] Chisa Itoh,[b] and Hitoshi Miyasaka,*[a,b]

[a] Institute for Materials Research, Tohoku University, 2-1-1 Katahira, Aoba-ku, Sendai 980-8577, Japan

[b] Department of Chemistry, Graduate School of Science, Tohoku University, 6-3 Aramaki-Aza-Aoba, Aoba-ku, Sendai 980-8578, Japan

Corresponding author*

Prof. Dr. Hitoshi Miyasaka

Institute for Materials Research

Tohoku University

2–1–1 Katahira, Aoba-ku, Sendai, Miyagi 980-8577, Japan

E-mail: hitoshi.miyasaka.e7@tohoku.ac.jp

Tel: +81-22-215-2030

FAX: +81-22-215-2031

■ Contents for SI

Table S1. Crystallographic Data.

	2Cl4OH·2THF	**3F4OH**·4THF	**3Cl4OH**·2THF	**3Br4OH**·4THF	**3F2OH**	**4F2OH**
formula	$C_{44}H_{48}Cl_4O_{16}Ru_2$	$C_{52}H_{64}F_4O_{18}Ru_2$	$C_{44}H_{48}Cl_4O_{16}Ru_2$	$C_{53}H_{64}Br_4O_{18}Ru_2$	$C_{36}H_{32}F_4O_{14}Ru_2$	$C_{36}H_{32}F_4O_{14}Ru_2$
formula weight	1176.76	1255.17	1176.76	1498.81	966.75	966.75
crystal system	monoclinic	orthorhombic	monoclinic	orthorhombic	triclinic	monoclinic
space group	$P2_1/c$	*Pbca*	$P2_1/n$	*Pbca*	$P\bar{1}$	$P2_1/c$
a / Å	13.7138(13)	14.2350(4)	13.9686(4)	17.0102(6)	8.0723(5)	9.4838(5)
b / Å	19.4669(11)	18.3819(5)	10.5955(3)	18.1666(4)	10.5927(9)	19.1954(10)
c / Å	8.4058(9)	20.2770(6)	15.9363(6)	18.4141(5)	11.6969(6)	10.1612(5)
α / deg	90	90	90	90	86.587(6)	90
β / deg	91.348(9)	90	93.675(3)	90	78.313(5)	103.587(6)
γ / deg	90	90	90	90	70.144(7)	90
V / Å^3	2243.4(3)	5305.8(3)	2353.79(13)	5690.3(3)	921.16(12)	1798.03(17)
Z	2	4	2	4	1	2
crystal size / mm^3	0.06×0.13×0.15	0.09×0.12×0.12	0.03×0.12×0.27	0.15×0.24×0.27	0.02×0.07×0.17	0.18×0.17×0.02
T / K	98(1)	93(1)	93(1)	102(1)	102(1)	102(1)
D_{calc} / g·cm^{-3}	1.742	1.571	1.660	1.750	1.743	1.786
F_{000}	1192.00	2576.00	1192.00	2992.00	484.00	968.00
λ / Å	0.71073	0.71073	0.71073	0.71073	0.71073	0.71073
μ(Mo Kα) / cm^{-1}	9.850	6.570	9.390	34.100	9.090	9.320
data measured	18257	42242	18554	44345	8509	11341
data unique	4990	6087	5390	6528	4039	4040
R_{int}	0.1120	0.0352	0.0258	0.0404	0.1465	0.0269
no. of observations	4990	6087	5390	6528	4039	4040
no. of variables	301	439	337	392	255	265
$R1$ ($I > 2.00\sigma(I)$)[a]	0.0950	0.0351	0.0288	0.0432	0.0703	0.0242
R (all reflections)[a]	0.1627	0.0515	0.0354	0.0496	0.1059	0.0286
$wR2$ (all reflections)[b]	0.2871	0.0850	0.0725	0.1030	0.2351	0.0599
GOF	1.046	1.036	1.017	1.210	1.117	1.067
CCDC No.	2394123	2394124	2394125	2394126	2394127	2394128

[a] $R1 = R = \Sigma||F_o|-|F_c||/\Sigma|F_o|$. [b] $wR2 = [\Sigma w(F_o^2-F_c^2)^2/\Sigma w(F_o^2)^2]^{1/2}$

Table S1 (continue). Crystallographic Data.

	4Cl2OH	**4Me2OH**	**5Cl2OH**	**5Br2OH**	**5Me2OH**
formula	$C_{36}H_{32}Cl_4O_{14}Ru_2$	$C_{40}H_{44}O_{14}Ru_2$	$C_{36}H_{32}Cl_4O_{14}Ru_2$	$C_{36}H_{32}Br_4O_{14}Ru_2$	$C_{40}H_{44}O_{14}Ru_2$
formula weight	1032.56	950.89	1032.55	1210.39	950.89
crystal system	monoclinic	triclinic	triclinic	triclinic	triclinic
space group	*C*2/*m*	*C*2/*m*	*P*–1	*P*–1	*P*–1
a / Å	13.1252(6)	12.9788(6)	8.8418(5)	9.1173(5)	8.8102(4)
b / Å	21.4303(8)	21.3992(9)	10.0803(5)	10.0764(4)	10.0823(5)
c / Å	9.2625(5)	9.2616(4)	11.1109(5)	11.2003(5)	11.2361(5)
α / deg	90	90	70.742(4)	70.963(4)	70.954(4)
β / deg	109.540(5)	104.507(4)	88.958(4)	89.019(4)	88.666(4)
γ / deg	90	90	81.456(4)	81.985(4)	80.302(4)
V / Å^3	2455.3(2)	2490.27(19)	924.00(8)	962.75(8)	929.41(8)
Z	2	2	1	1	1
crystal size / mm^3	0.26×0.21×0.09	0.10×0.05×0.05	0.03×0.08×0.36	0.03×0.16×0.17	0.05×0.02×0.01
T / K	102(1)	102(1)	103(1)	103(1)	102(1)
D_{calc} / g·cm^{-3}	1.533	1.268	1.856	2.088	1.699
F_{000}	1144.00	968.00	516.00	588.00	484.00
λ / Å	0.71073	0.71073	0.71073	0.71073	0.71073
μ(Mo Kα) / cm^{-1}	8.960	6.760	11.780	50.010	8.850
data measured	9160	8998	10205	10840	12170
data unique	2702	2726	4164	5567	4455
R_{int}	0.0271	0.0330	0.0283	0.0222	0.0836
no. of observations	2702	2726	4164	4318	4455
no. of variables	157	161	255	255	260
*R*1 ($I > 2.00\sigma(I)$)[a]	0.0601	0.0502	0.0237	0.0268	0.0471
R (all reflections)[a]	0.0781	0.0616	0.0265	0.0319	0.0686
*wR*2 (all reflections)[b]	0.2144	0.1727	0.0610	0.0660	0.1130
GOF	1.099	1.075	1.057	1.041	1.005
CCDC No.	2394129	2394130	2394131	2394132	2394133

[a] $R1 = R = \Sigma||F_o|-|F_c||/\Sigma|F_o|$. [b] $wR2 = [\Sigma w(F_o^2-F_c^2)^2/\Sigma w(F_o^2)^2]^{1/2}$

Table S1 (continue). Crystallographic Data.

	ht-4F2OH	**ht-4Cl2OH**	**ht-4Me2OH**	**ht-4OMe2OH**	**ht-4CF$_3$2OH**	**ht-5Me2OH**
formula	$C_{40}H_{30}F_{14}O_{12}Ru_2$	$C_{40}H_{30}Cl_2F_{12}O_{12}Ru_2$	$C_{42}H_{36}F_{12}O_{12}Ru_2$	$C_{42}H_{36}F_{12}O_{14}Ru_2$	$C_{42}H_{30}F_{18}O_{12}Ru_2$	$C_{42}H_{36}F_{12}O_{12}Ru_2$
formula weight	1170.78	1203.68	1162.85	1194.85	1270.80	1162.85
crystal system	monoclinic	monoclinic	monoclinic	monoclinic	triclinic	monoclinic
space group	$P2_1/n$	$P2_1/n$	$P2_1/n$	$C2/c$	$P\bar{1}$	$C2/c$
a / Å	11.0125(3)	10.9776(5)	11.0636(5)	23.8874(17)	9.7520(5)	25.9938(10)
b / Å	14.1717(3)	14.0906(5)	14.1368(5)	9.9299(4)	10.3379(6)	8.5471(4)
c / Å	14.5066(4)	14.7802(7)	14.7467(7)	23.6731(19)	11.7134(5)	21.7511(9)
α / deg	90	90	90	90	91.483(4)	90
β / deg	110.034(3)	107.382(5)	107.557(5)	126.003(11)	105.485(4)	96.794(4)
γ / deg	90	90	90	90	92.535(4)	90
V / Å^3	2126.99(10)	2181.81(17)	2199.00(17)	4542.7(7)	1136.04(10)	4798.5(4)
Z	2	2	2	4	1	4
crystal size / mm^3	0.53×0.35×0.27	0.26×0.15×0.12	0.27×0.24×0.05	0.31×0.11×0.09	0.19×0.09×0.07	0.21×0.13×0.06
T / K	102(1)	102(1)	102(1)	102(1)	102(1)	102(1)
D_{calc} / g·cm^{-3}	1.828	1.832	1.756	1.747	1.857	1.610
F_{000}	1160.00	1192.00	1160.00	2384.00	628.00	2320.00
λ / Å	0.71073	0.71073	0.71073	0.71073	0.71073	0.71073
μ(Mo Kα) / cm^{-1}	8.340	9.280	8.000	7.800	8.010	7.330
data measured	18813	15083	14879	13914	10585	12790
data unique	5120	4637	5570	5390	4823	4979
R_{int}	0.0279	0.0351	0.0229	0.0713	0.0893	0.0774
no. of observations	5120	4637	5570	5390	4823	4979
no. of variables	308	374	337	318	346	309
$R1$ ($I > 2.00\sigma(I)$)[a]	0.0309	0.0296	0.0338	0.0560	0.0740	0.0497
R (all reflections)[a]	0.0362	0.0350	0.0384	0.0735	0.1052	0.0587
$wR2$ (all reflections)[b]	0.0784	0.0732	0.0823	0.1457	0.1864	0.1480
GOF	1.025	1.117	1.094	1.056	1.013	1.042
CCDC No.	2394134	2394135	2394136	2394137	2394138	2394139

[a] $R1 = R = \Sigma||F_o|-|F_c||/\Sigma|F_o|$. [b] $wR2 = [\Sigma w(F_o^2-F_c^2)^2/\Sigma w(F_o^2)^2]^{1/2}$

Table S2. Magnetic parameters of $\{Ru_2^{II,II}(OH\text{-}X\text{-}ArCO_2)_4(THF)_2\}$ compounds obtained from the best-fit of χ vs. T data using a Curie equation for $S = 1$ with $g = 2.00$ (fix) and $zJ' = 0$ (fix).

Compound	D [K]	χ_{TIP} [10^{-6} cm^3 mol^{-1}]	ρ [10^{-3}]
2Cl4OH	343.5(9)	44(3)	112.9(6)
3F4OH	338.1(11)	47(8)	56.7(3)
3Cl4OH	387.8(3)	25.7(19)	9.02(11)
3Br4OH	337.2(14)	170(10)	21.6(4)
3F2OH	383.1(9)	24(5)	3.6(2)
4F2OH	368.7(9)	36(6)	1.9(2)
4Cl2OH	365(5)	69(30)	168.4(12)
4Me2OH	351(3)	100(17)	92.3(8)
4OMe2OH	403(5)	93(15)	65.7(5)
5Cl2OH	368.1(6)	54(4)	1.37(16)
5Br2OH	369.1(13)	40(11)	4.79(13)
5Me2OH	392.1(5)	72(3)	4.27(11)
ht-4F2OH	411.4(9)	64(6)	3.18(16)
ht-4Cl2OH	382.2(5)	17(3)	1.70(12)
ht-4Me2OH	401.3(18)	90(11)	34.8(4)
ht-4OMe2OH	386.0(12)	81(8)	16.3(3)
ht-4CF$_3$2OH	462(4)	66(21)	57.8(6)
ht-5Me2OH	452(3)	47(18)	11.4(5)

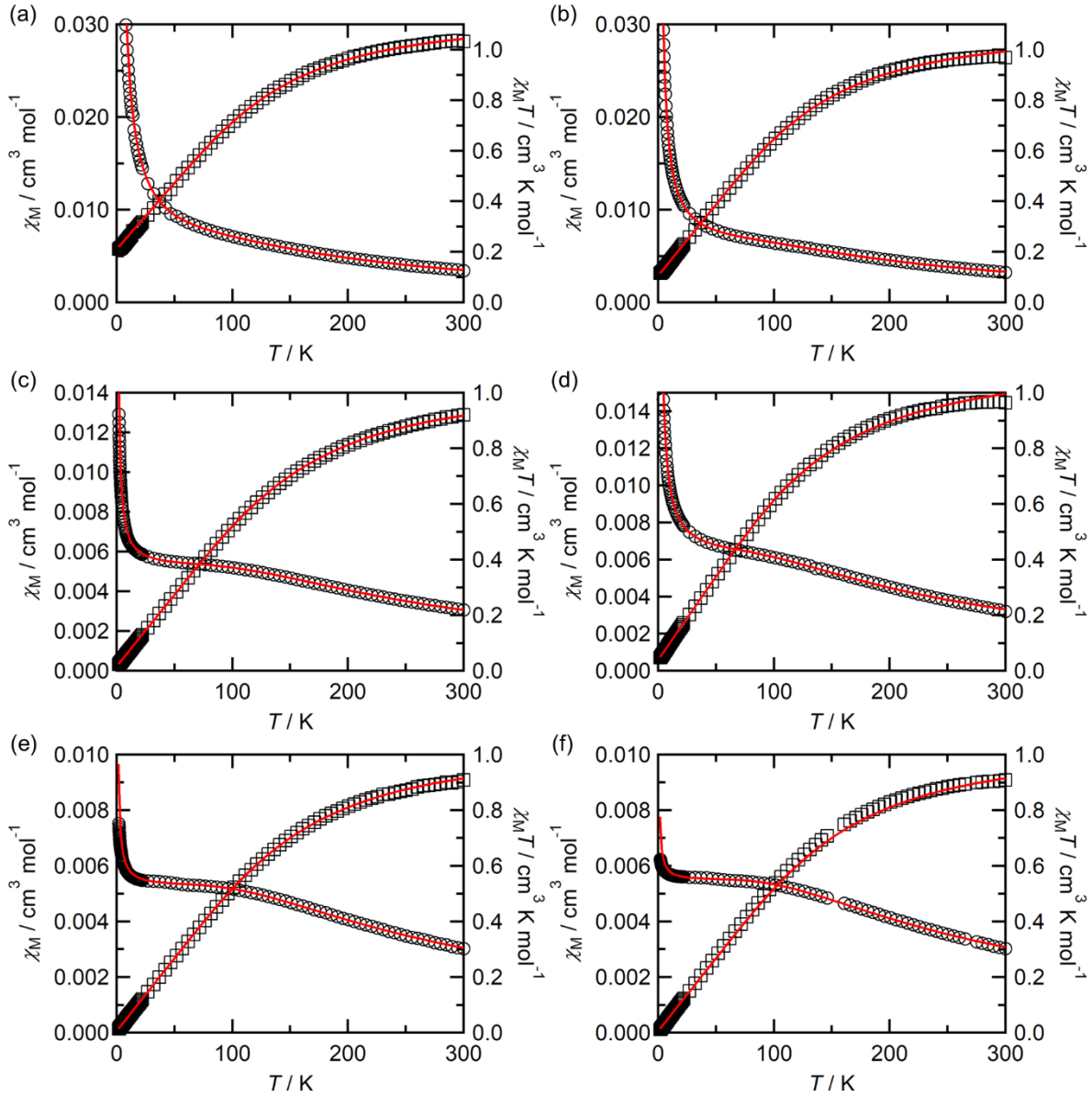

Fig. S1. Temperature dependence of χ (○) and χT (□) for **2Cl4OH**, (a), **3F4OH** (b), **3Cl4OH** (c), **3Br4OH** (d), **3F2OH** (e), and **4F2OH** (f), where the red solid lines represent simulated curves based on a Curie paramagnetic model with $S = 1$ taking into account zero-field splitting (D), temperature-independent paramagnetism (χ_{TIP}), and impurity with $S = 3/2$ (ρ).

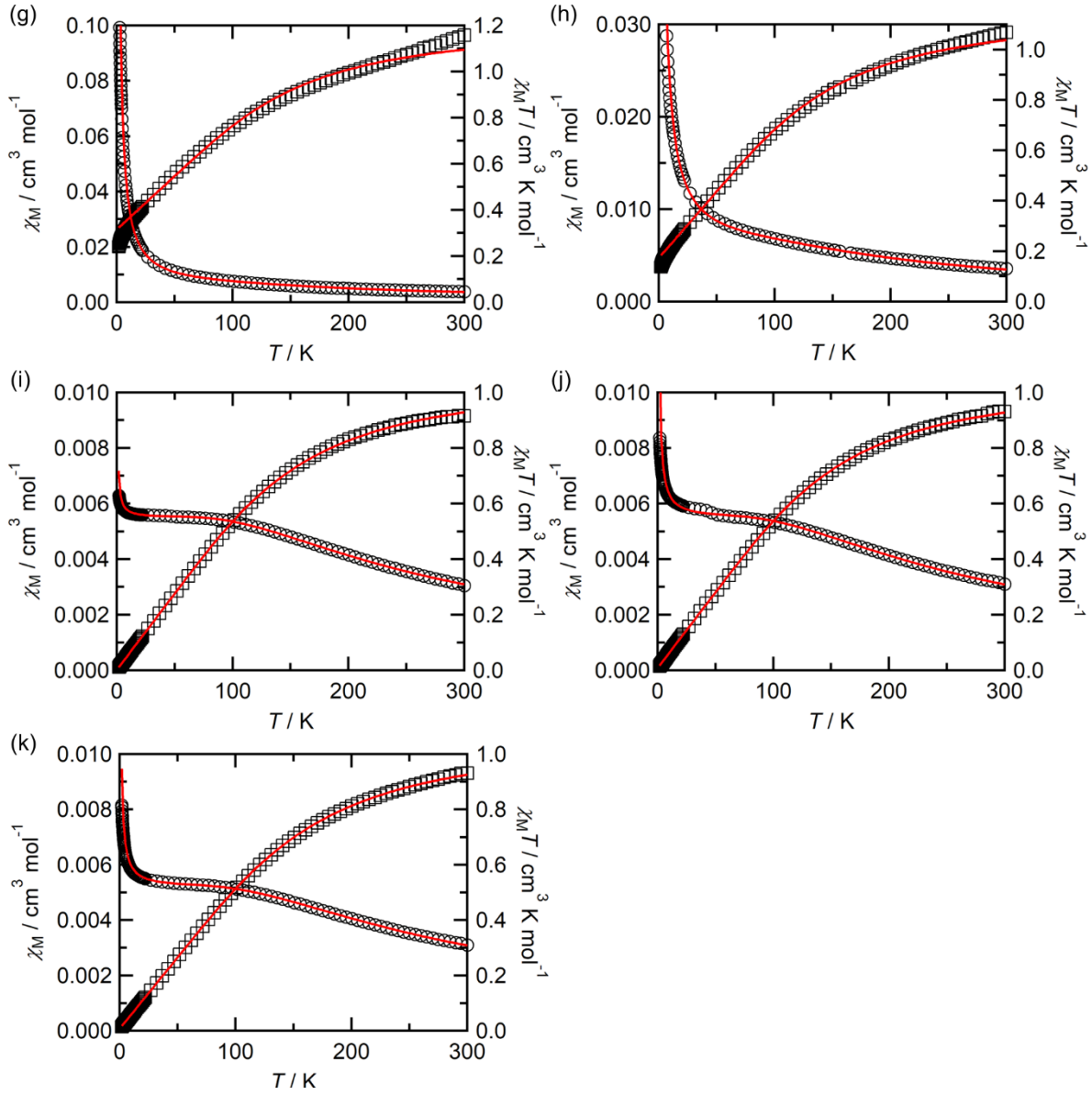

Fig. S1 (continue). Temperature dependence of χ (○) and χT (□) for **4Cl2OH**, (g), **4Me2OH** (h), **5Cl2OH** (i), **5Br2OH** (j), and **5Me2OH** (k), where the red solid lines represent simulated curves based on a Curie paramagnetic model with S = 1 taking into account zero-field splitting (D), temperature-independent paramagnetism (χ_{TIP}), and impurity with S = 3/2 (ρ).

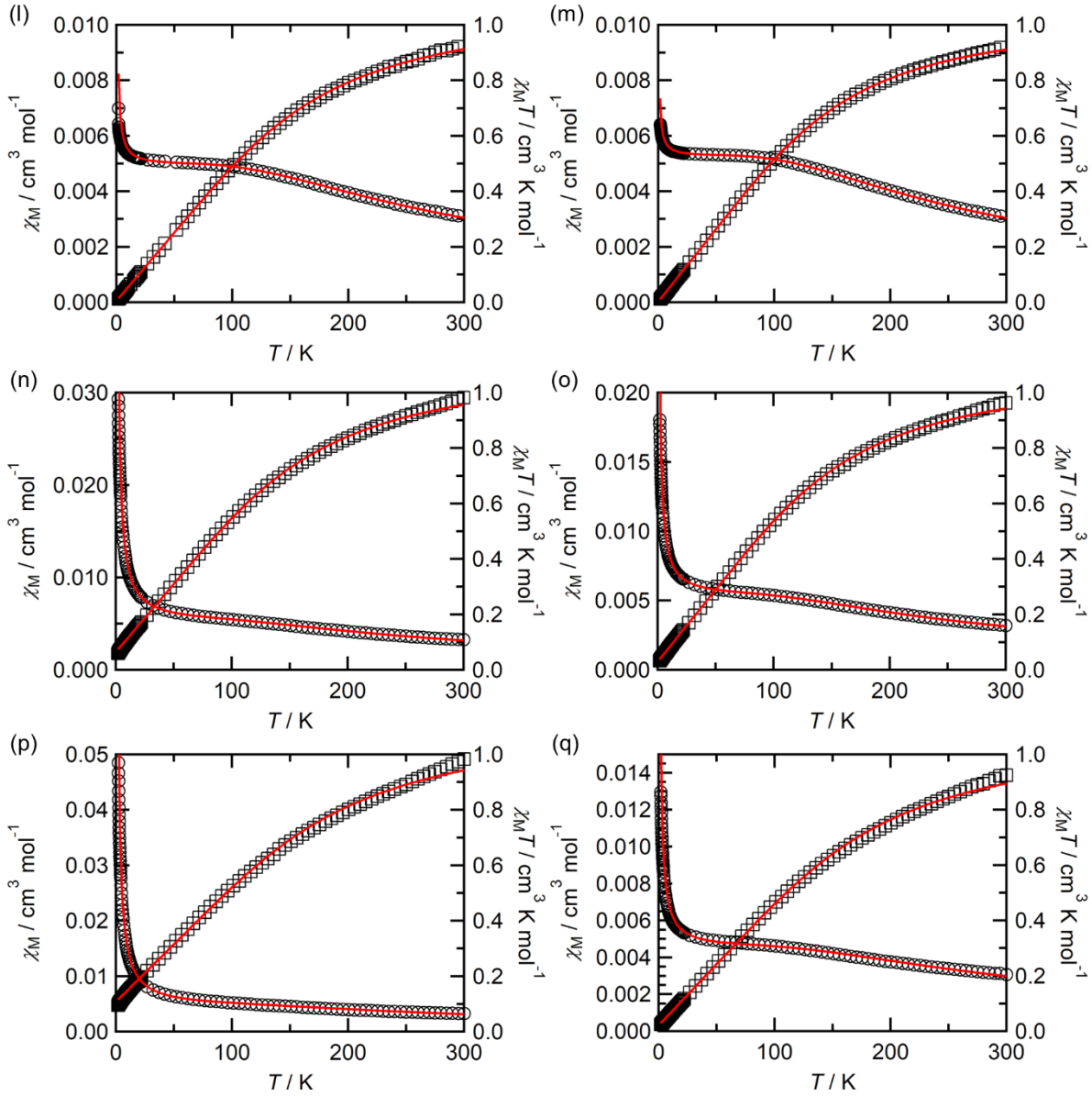

Fig. S1 (continue). Temperature dependence of χ (○) and χT (□) for **ht-4F2OH**, (l), **ht-4Cl2OH** (m), **ht-4Me2OH** (n), **ht-4OMe2OH** (o), **ht-4CF$_3$2OH** (p), and **ht-5Me2OH** (q), where the red solid lines represent simulated curves based on a Curie paramagnetic model with $S = 1$ taking into account zero-field splitting (D), temperature-independent paramagnetism (χ_{TIP}), and impurity with $S = 3/2$ (ρ).

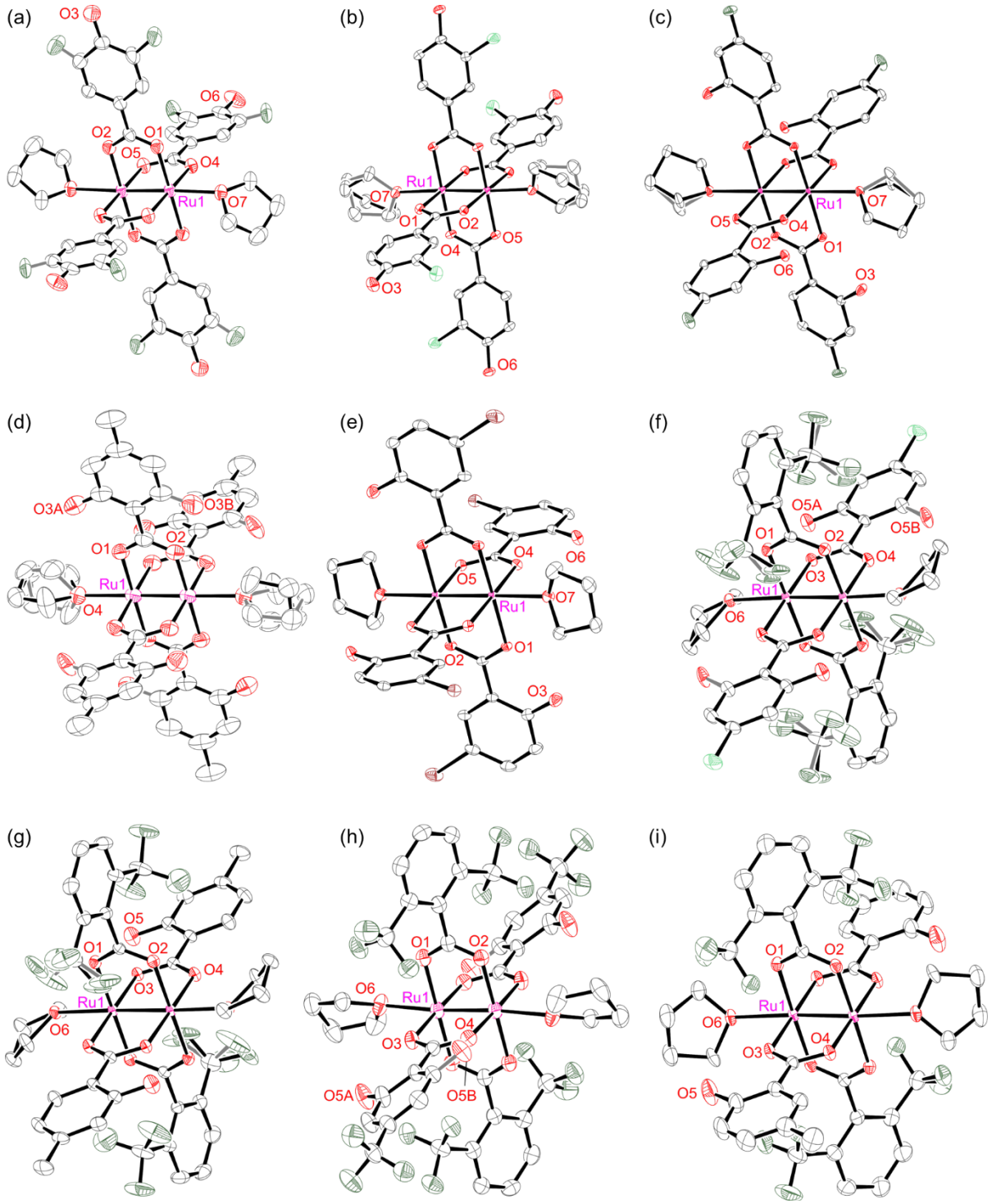

Fig. S2. ORTEP drawings of for **3F4OH**, (a), **3Cl4OH** (b), **4F2OH** (c), **4Me2OH** (d), **5Br2OH** (e), **ht-4Cl2OH** (f), **ht-4Me2OH** (g), **ht-4CF$_3$2OH** (h), and **ht-5Me2OH** (i), Red, gray, green, light green, purple, and pink represent O, C, F, Cl, Br, and Ru, respectively. The grey bonds represent disordered atomic positions. Displacement ellipsoids are drawn at a 50% probability level. Hydrogen atoms and crystallization solvents are omitted for clarity.

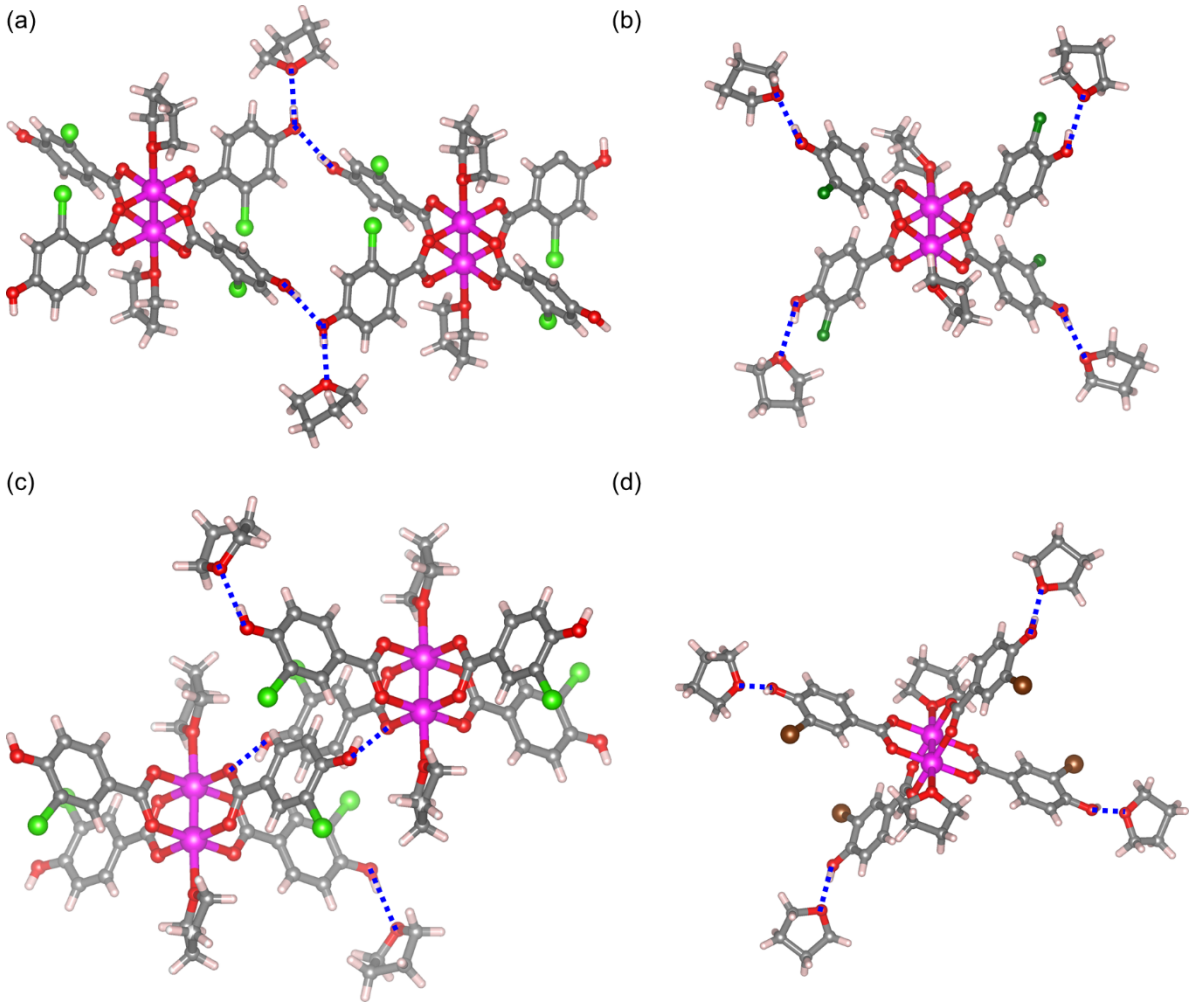

Fig. S3. Molecular structures focused on intermolecular hydrogen bond; **2Cl4OH**, (a), **3F4OH** (b), **3Cl4OH** (c), and **3Br4OH** (d). Red, gray, green, light green, purple, light brown, and pink represent O, C, F, Cl, Br, H, and Ru, respectively. Intermolecular hydrogen bond is depicted in blue dotted line.

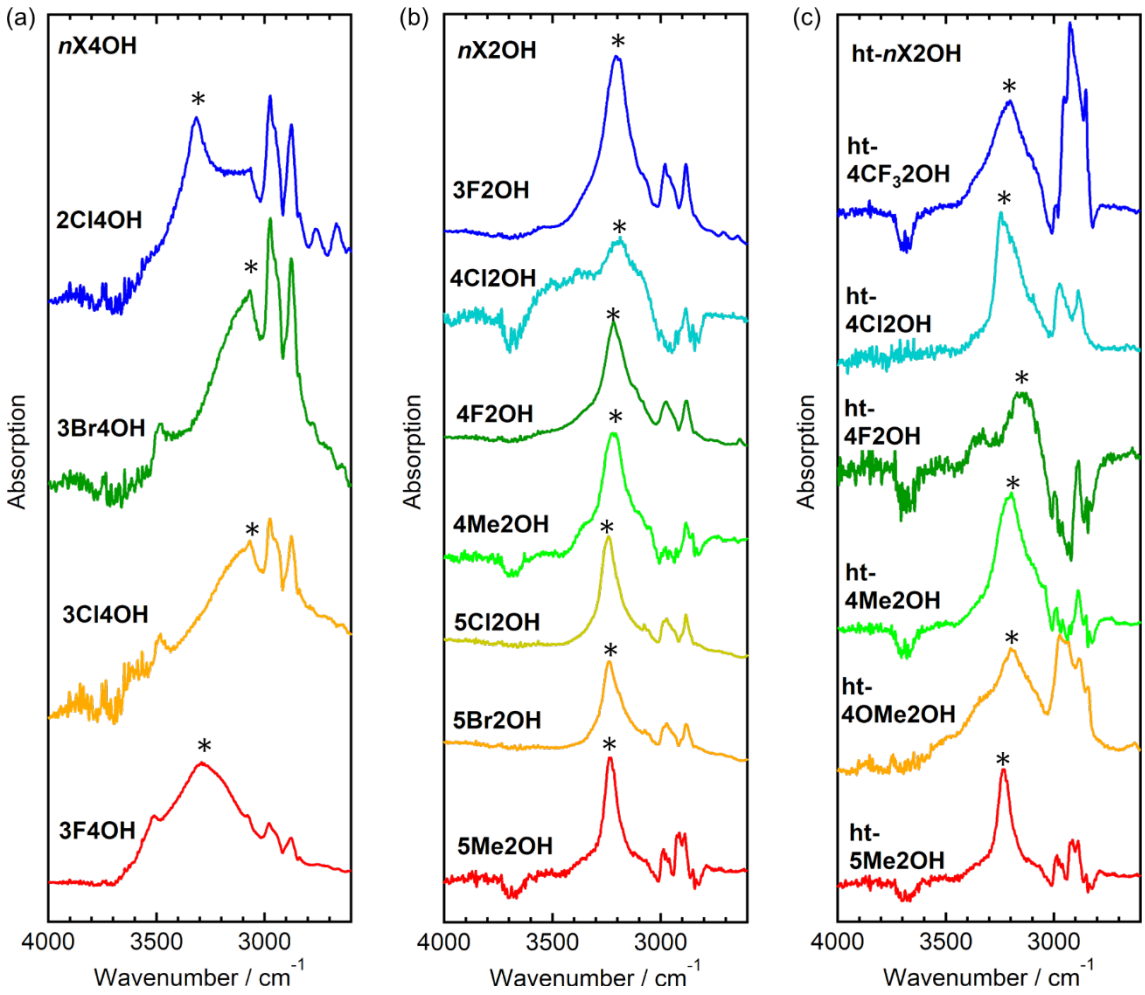

Fig. S4. IR spectra in the OH stretching region, where the peak positions are indicated by asterisks (*), ***n*X4OH** (a), ***n*X2OH** (b), and **ht-*n*X2OH** (c).

Determination of Hammett constants for *ortho*-substituents

The Hammett constants are only known for the *m*- and *p*- substituents, though we experimentally determined the Hammett constant for the *o*-F, *o*-Cl, and *o*-OH group that can be used for the prediction of $E_{1/2}$ value of [Ru_2] from the Hammett analyses. To determine σ_o, the error for the least-squares linear fit in the plot of $E_{1/2}$ vs. $\Sigma(\alpha\sigma_m + \beta\sigma_p + \gamma\sigma_o)$ was minimized for the respective series, providing σ_o values of 0.217, 0.272, and 0.667 for F, Cl, and OH series, respectively.[1,2]

Similarly, Hammett constants for the *o*-Me, *o*-OMe, and *o*-CF_3 groups were determined as −0.070, −0.397, and 0.50, respectively. The $E_{1/2}$ values of previously reported [Ru_2] compounds were used, listed in Table S3 and S4. [3,4]

Table S3. Electrochemical data[a] and the HOMO level calculated by density functional theory of reported $[Ru_2(R_nArCO_2)_4(THF)_2]$.

	R	$E_{1/2}$ / mV	HOMO energy / eV	pK_a of benzoic acid[b]	$\Sigma(\alpha\sigma_m + \beta\sigma_p)$[c]	$\Sigma(\alpha\sigma_m + \beta\sigma_p + \gamma\sigma_o)$[c,d]	Ref
1	**3,4,5-F_3**	274	−5.0678	3.46	0.736	0.736	1,5
2	**3,5-F_2**	178	−4.9566	3.52	0.674	0.674	1,5
3	**3,4-F_2**	144	−4.7677	3.80	0.399	0.399	1,5
4	***m*-F**	42	−4.4218	3.86	0.337	0.337	1,5
5	***p*-F**	−39	−4.5114	4.14	0.062	0.062	1,5
6	**3,4,5-Cl_3**	266	−5.0692	3.23	0.973	0.973	1
7	**3,5-Cl_2**	221	−4.9391	3.46	0.746	0.746	1
8	**3,4-Cl_2**	112	−4.7759	3.60	0.600	0.600	1
9	***m*-Cl**	86	−4.5323−	3.83	0.373	0.373	1
10	***p*-Cl**	22	−4.5048	3.98	0.227	0.227	1
11	***m*-Me**	−99	−4.1372	4.27	−0.069	−0.069	3
12	***p*-Me**	−116	−4.0401	4.37	−0.170	−0.170	3
13	***p*-CF_3**	116	−4.7454	3.69	0.540	0.540	6
14	**H**	60	−4.1326	4.20	0	0	6
15	***p*-Ph**	38	−4.2673	4.19	0.144	0.144	6
16	***p*-OMe**	−184	−3.9318	4.47	−0.268	−0.268	6
17	***p*-CHO**	67	−4.8412	3.78	0.420	0.420	7
18	**F_5**	358	−5.1144	1.60	0.736	1.170	1,5
19	**2,3,5,6-F_4**	360	−4.8518	1.66	0.674	1.108	1,5
20	**2,3,4,5-F_4**	315	−5.0578	2.53	0.736	0.953	1,5
21	**2,3,6-F_3**	336	−4.6502	2.00	0.337	0.771	1,5
22	**2,4,5-F_3**	214	−4.8893	2.87	0.399	0.616	1,5
23	**2,3,4-F_3**	209	−4.9432	2.87	0.399	0.616	1,5
24	**2,3,5-F_3**	225	−4.8785	2.59	0.674	0.891	1
25	**2,4,6-F_3**	172	−4.7424	2.28	0.062	0.496	1,5
26	**2,5-F_2**	99	−4.6401	2.93	0.337	0.554	1
27	**2,3-F_2**	93	−4.5223	2.93	0.337	0.554	1
28	**2,6-F_2**	51	−4.3242	2.34	0	0.434	1,5
29	**2,4-F_2**	35	−4.4874	3.21	0.062	0.399	1
30	***o*-F**	35	−4.1840	3.27	0	0.217	1,5
31	**2,3,4,5-Cl_4**	337	−5.0235	1.80	0.973	1.245	1
32	**2,3,5-Cl_3**	296	−4.9212	2.09	0.746	1.018	1
33	**2,3,4-Cl_3**	240	−5.1590	2.23	0.600	0.872	1
34	**2,4,5-Cl_3**	226	−4.9255	2.25	0.600	0.872	1
35	**2,5-Cl_2**	167	−4.5906	2.51	0.373	0.645	1
36	**2,3-Cl_2**	154	−4.5516	2.53	0.373	0.645	1
37	**2,6-Cl_2**	130	−4.4512	1.69	0	0.544	1
38	**2,4-Cl_2**	112	−4.7759	3.60	0.600	0.600	1
39	***o*-Cl**	41	−4.1677	2.94	0	0.272	1
40	***o*-Me**	−94	−4.1617	3.95	0	−0.070	3
41	**2,4,5-Me_3**	−179	−3.9038	4.24	−0.239	−0.309	8
42	***o*-OMe**	−228	−3.7270	4.09	0	−0.397	4
43	**4-Cl-2-OMe**	−131	−4.1323	3.86	0.227	−0.170	4
44	**4-F-2-OMe**	−178	−4.0866	4.03	0.062	−0.335	4
45	***o*-CF_3**	126	−4.3821	3.20	0	0.500	3

[a]Measured in THF containing 0.1 M *n*-$Bu_4N(PF_6)$ under N_2 (mV vs. Ag/Ag^+). The ferrocene/ferrocenium couple, Fc/Fc^+ = 213 mV, was observe at the same condition. [b]Predicted values calculated using Advanced Chemistry Development (ACD/Labs) Software V11.02, which were obtained from SciFinder-*n* database. [c]Hammett constants σ_m and σ_p were taken from ref. 9. [d]Hammett constants σ_o were taken from ref. 1.

Table S4. Electrochemical data[a] and the HOMO level calculated by density functional theory of reported $[Ru_2\{2,6\text{-}(CF_3)_2ArCO_2\}_2(R_nArCO_2)_2(THF)_2]$.

	R	$E_{1/2}$ / mV	HOMO energy / eV	pK_a of benzoic acid[b]	$\Sigma(\alpha\sigma_m + \beta\sigma_p)$[c]	$\Sigma(\alpha\sigma_m + \beta\sigma_p + \gamma\sigma_o)$[c,d]	Ref
46	***o*-OH**	291	−4.5900	3.01	0	0.689	2
47	***m*-OH**	76	−4.3680	4.08	0.121	0.121	2
48	***p*-OH**	−18	−4.3214	4.57	−0.370	−0.370	2
49	**2,3-(OH)$_2$**	240	−4.6716	2.96	0.121	0.810	2
50	**2,4-(OH)$_2$**	192	−4.5642	3.32	−0.370	0.319	2
51	**2,5-(OH)$_2$**	280	−4.6746	3.01	0.121	0.810	2
52	**2,6-(OH)$_2$**	432	−4.8540	1.30	0	1.378	2
53	**3,4-(OH)$_2$**	18	−4.3503	4.45	−0.248	−0.248	2
54	***p*-CF$_3$**	237	−4.6602	3.69	0.540	0.540	6
55	***p*-Cl**	176	−4.6208	3.98	0.227	0.227	6
56	***p*-F**	160	−4.5658	4.14	0.062	0.062	6
57	**H**	108	−4.400	4.20	0	0	6
58	***p*-Ph**	112	−4.4025	4.19	0.009	0.009	6
59	***p*-Me**	83	−4.3046	4.37	−0.170	−0.170	6
60	***p*-OMe**	42	−4.2335	4.47	−0.268	−0.268	6
61	***p*-CHO**	185	−4.6820	3.78	0.420	0.420	7
62	**2,3,5,6-F$_4$**	314	−4.7960	1.66	0.674	1.108	10

[a]Measured in THF containing 0.1 M *n*-$Bu_4N(PF_6)$ under N_2 (mV vs. Ag/Ag^+). The ferrocene/ferrocenium couple, Fc/Fc^+ = 213 mV, was observe at the same condition. [b]Predicted values calculated using Advanced Chemistry Development (ACD/Labs) Software V11.02, which were obtained from SciFinder-*n* database. [c]Hammett constants σ_m and σ_p were taken from ref. 9. [d]Hammett constants σ_o were taken from ref. 1.

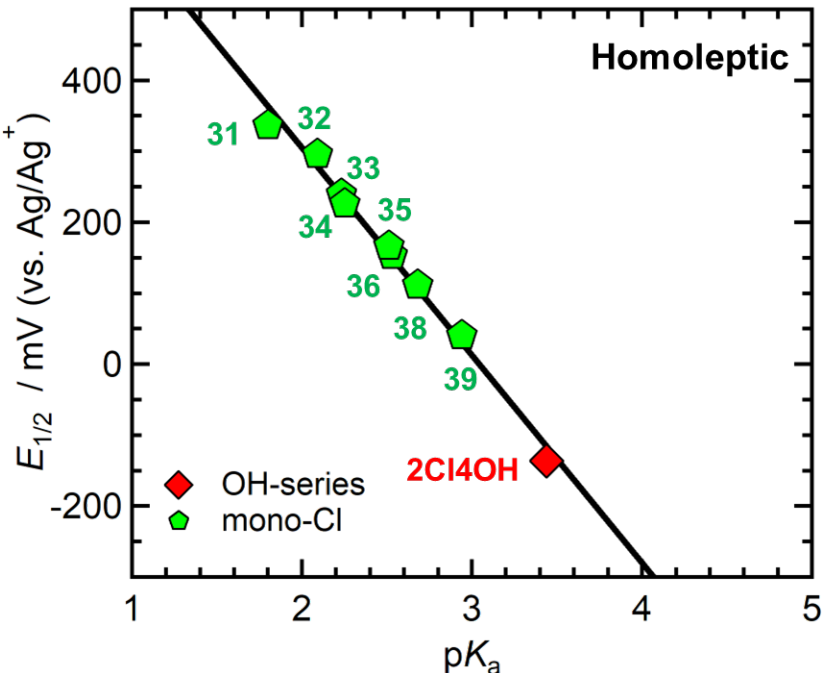

Fig. S5. Plot of half-wave redox potential ($E_{1/2}$) vs. pK_a for the corresponding benzoic acids in the homoleptic mono-Cl series of $[Ru_2(R_nArCO_2)_4(THF)_2]$. $E_{1/2}$ values are measured in THF with a Ag/Ag^+ reference electrode. Light green symbols represent the homoleptic compounds taken from ref. 1. The solid line represents the linear least-squares fitted line with an equation of $y = -292.61x + 890.2$ ($R^2 = 0.9895$). Definitions: $[Ru_2(R_nArCO_2)_4(THF)_2]$, R for **31**, 2,3,4,5-$Cl_4$; **32**, 2,3,5-$Cl_3$; **33**, 2,3,4-$Cl_3$; **34**, 2,4,5-$Cl_3$; **35**, 2,5-$Cl_2$; **36**, 2,3-$Cl_2$; **38**, 2,4-$Cl_2$; **39**, *o*-Cl.

Table S5. Estimated energy levels (eV) of π*- and δ*-characteristic orbitals for [$Ru_2^{II,II}$] complexes.

Electron character	Orbital character	2Cl4OH	3F4OH	3Cl4OH	3Br4OH
β	π*	−1.66017	−1.82262	−1.74942	−1.85201
	π*	−1.75405	−1.92031	−1.86861	−1.96494
	δ*	−4.15219	−4.34675	−4.30675	−4.38702
α	δ*	−4.57696	−4.77206	−4.73179	−4.81261
	π*	−4.81016	−4.98839	−4.90785	−5.02105
	π*	−4.93071	−5.10921	−5.04908	−5.14241

Electron character	Orbital character	3F2OH	4F2OH	4Cl2OH	4Me2OH
β	π*	−2.35814	−2.41583	−2.45148	−1.89609
	π*	−2.52767	−2.53447	−2.56658	−2.02017
	δ*	−4.97615	−4.99220	−5.00771	−4.43981
α	δ*	−5.39956	−5.41561	−5.4314	−4.86213
	π*	−5.49425	−5.57289	−5.60392	−5.04826
	π*	−5.70814	−5.72092	−5.74732	−5.19629

Electron character	Orbital character	5Cl2OH	5Br2OH	5Me2OH
β	π*	−2.49610	−2.52903	−2.03405
	π*	−2.60440	−2.63869	−2.15596
	δ*	−5.07629	−5.10894	−4.59982
α	δ*	−5.50106	−5.53344	−5.02268
	π*	−5.65018	−5.68419	−5.18105
	π*	−5.79276	−5.82650	−5.33343

Electron character	Orbital character	ht-4F2OH	ht-4Cl2OH	ht-4Me2OH	ht-4OMe2OH
β	π*	−2.19841	−2.14344	−1.97854	−1.93446
	π*	−2.27324	−2.23079	−2.04630	−2.00439
	δ*	−4.75982	−4.71329	−4.52852	−4.47900
α	δ*	−5.18268	−5.13615	−4.95084	−4.89996
	π*	−5.36473	−5.30677	−5.14758	−5.09996
	π*	−5.46160	−5.42160	−5.23112	−5.18023

Electron character	Orbital character	ht-4$CF_3$2OH	ht-5Me2OH
β	π*	−2.18099	−1.94235
	π*	−2.32494	−2.10834
	δ*	−4.76036	−4.55002
α	δ*	−5.18459	−4.97288
	π*	−5.33806	−5.08772
	π*	−5.50459	−5.30568

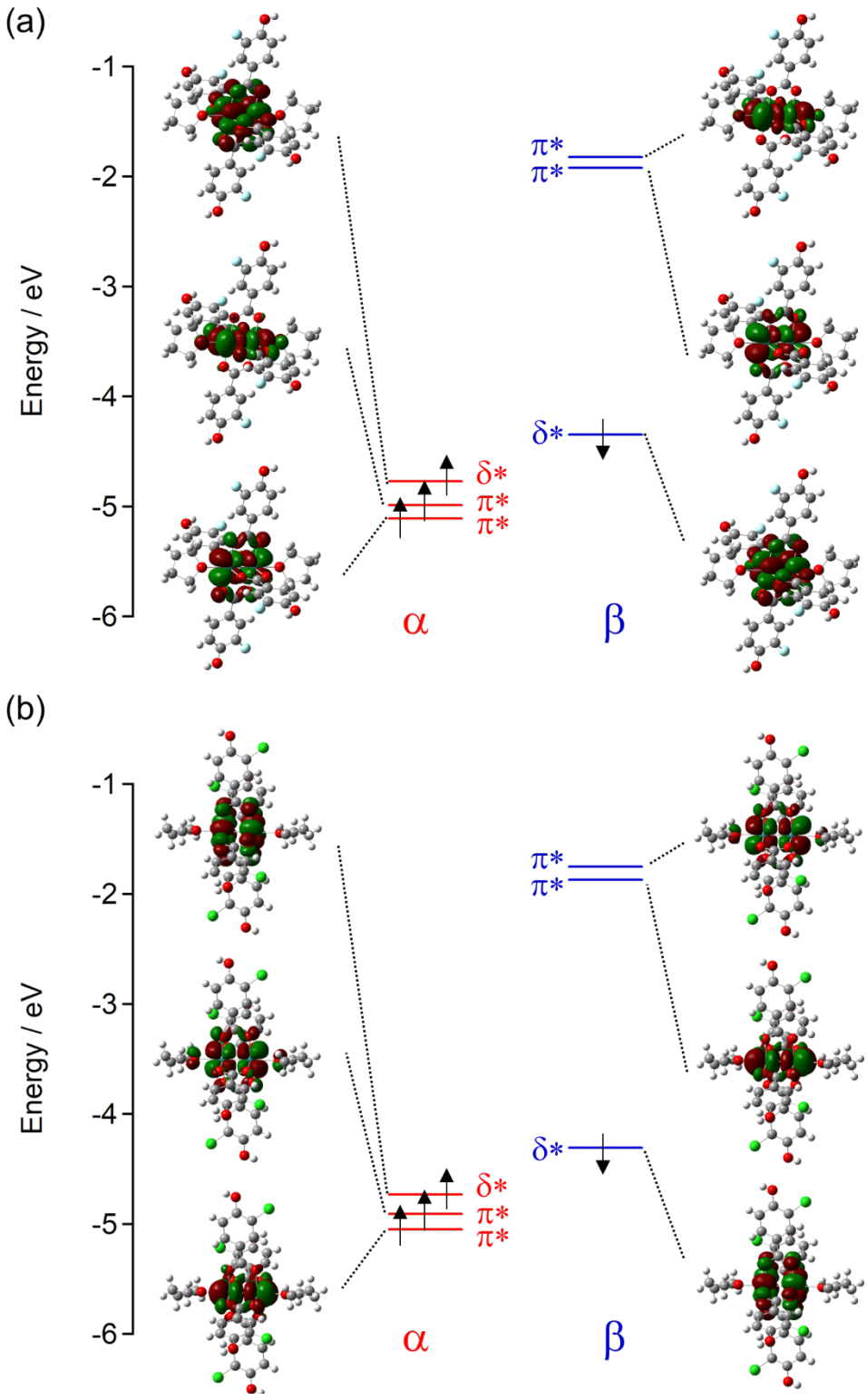

Fig. S6. Frontier orbitals associated with π* and δ* orbitals for **3F4OH** (a) and **3Cl4OH** (b), and their energy levels (eV), where δ* for β electron corresponds to HOMO level.

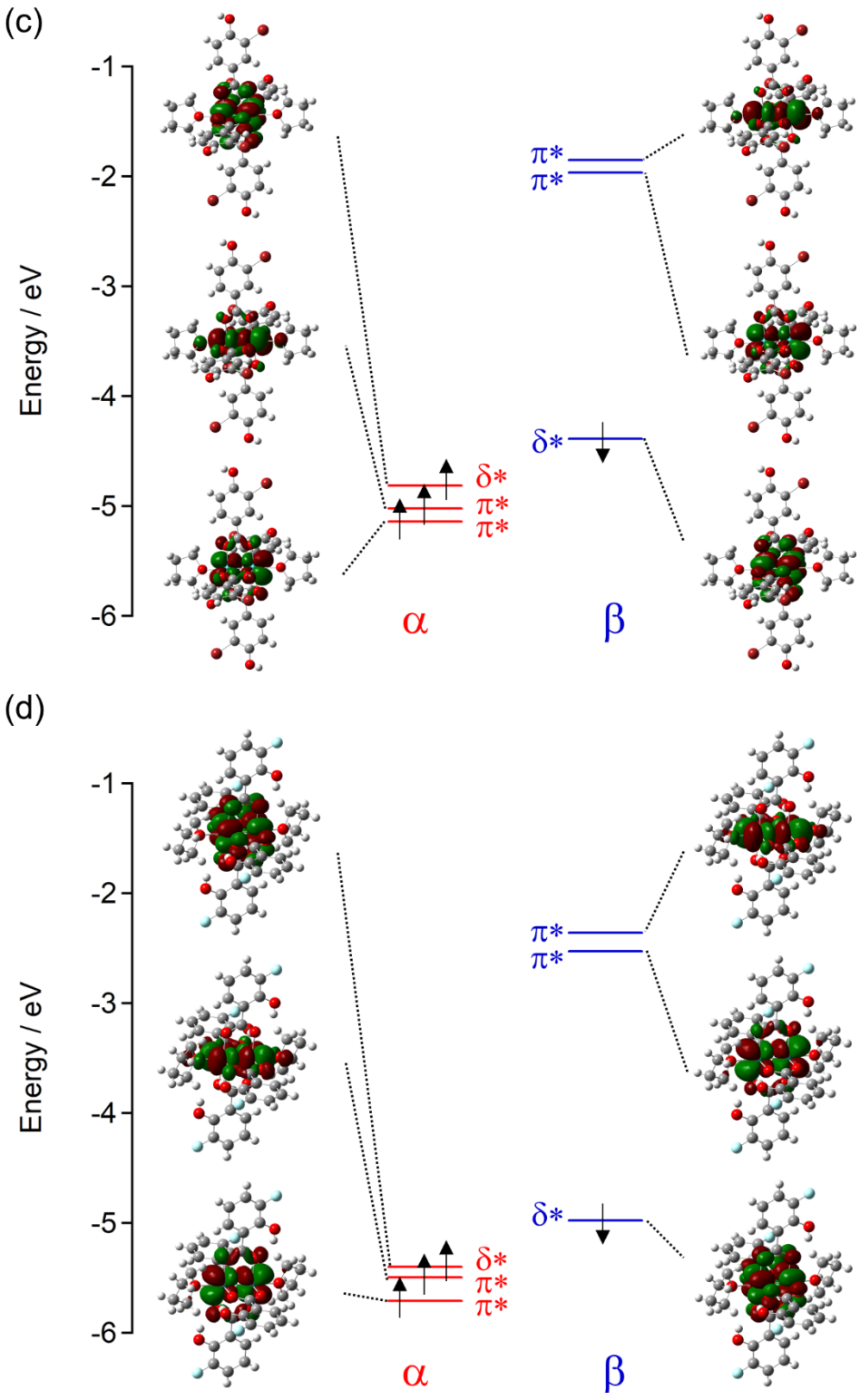

Fig. S6 (continued). Frontier orbitals associated with π* and δ* orbitals for **3Br4OH** (c) and **3F2OH** (d), and their energy levels (eV), where δ* for β electron corresponds to HOMO level.

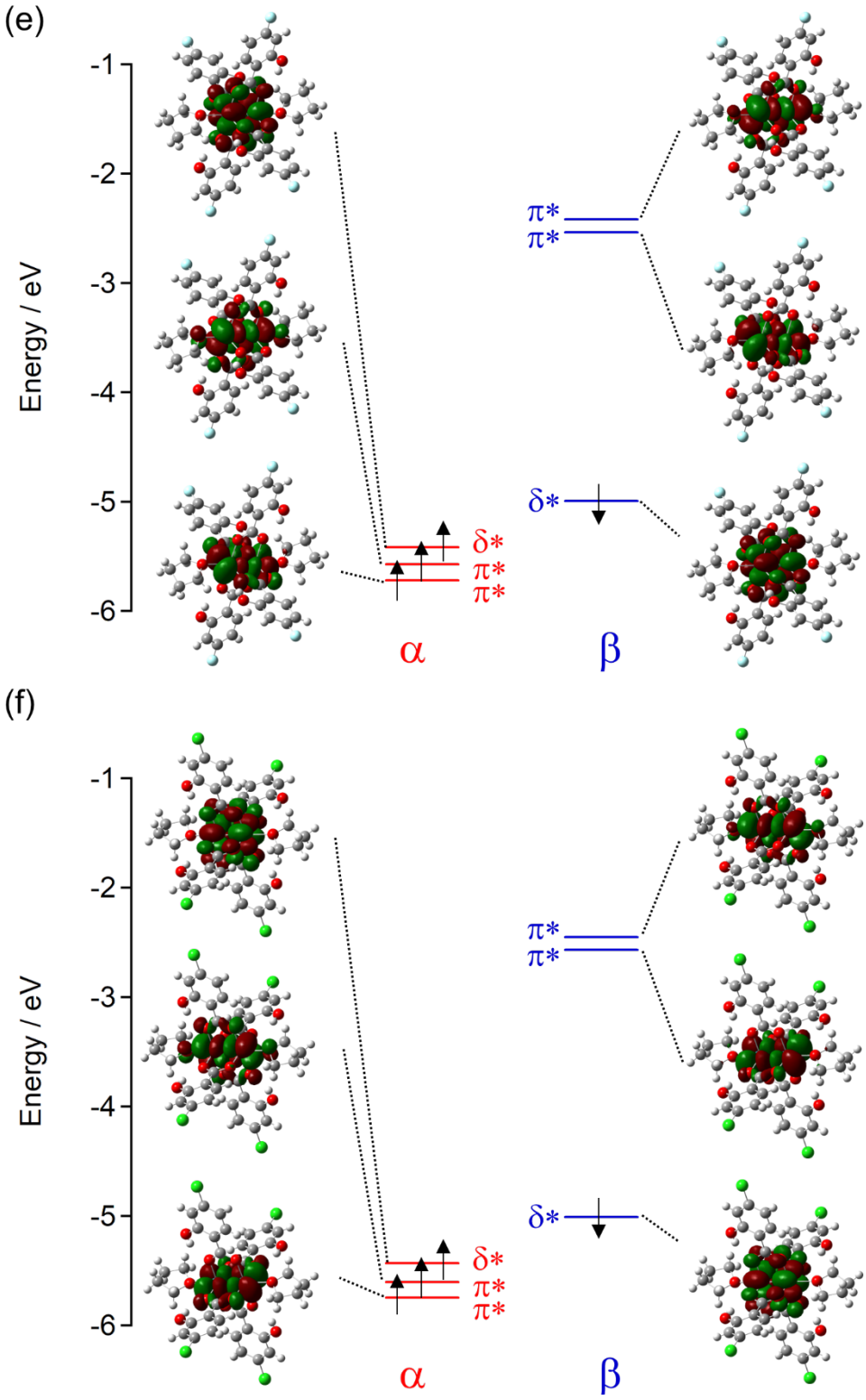

Fig. S6 (continued). Frontier orbitals associated with π* and δ* orbitals for **4F2OH** (e) and **4Cl2OH** (f), and their energy levels (eV), where δ* for β electron corresponds to HOMO level.

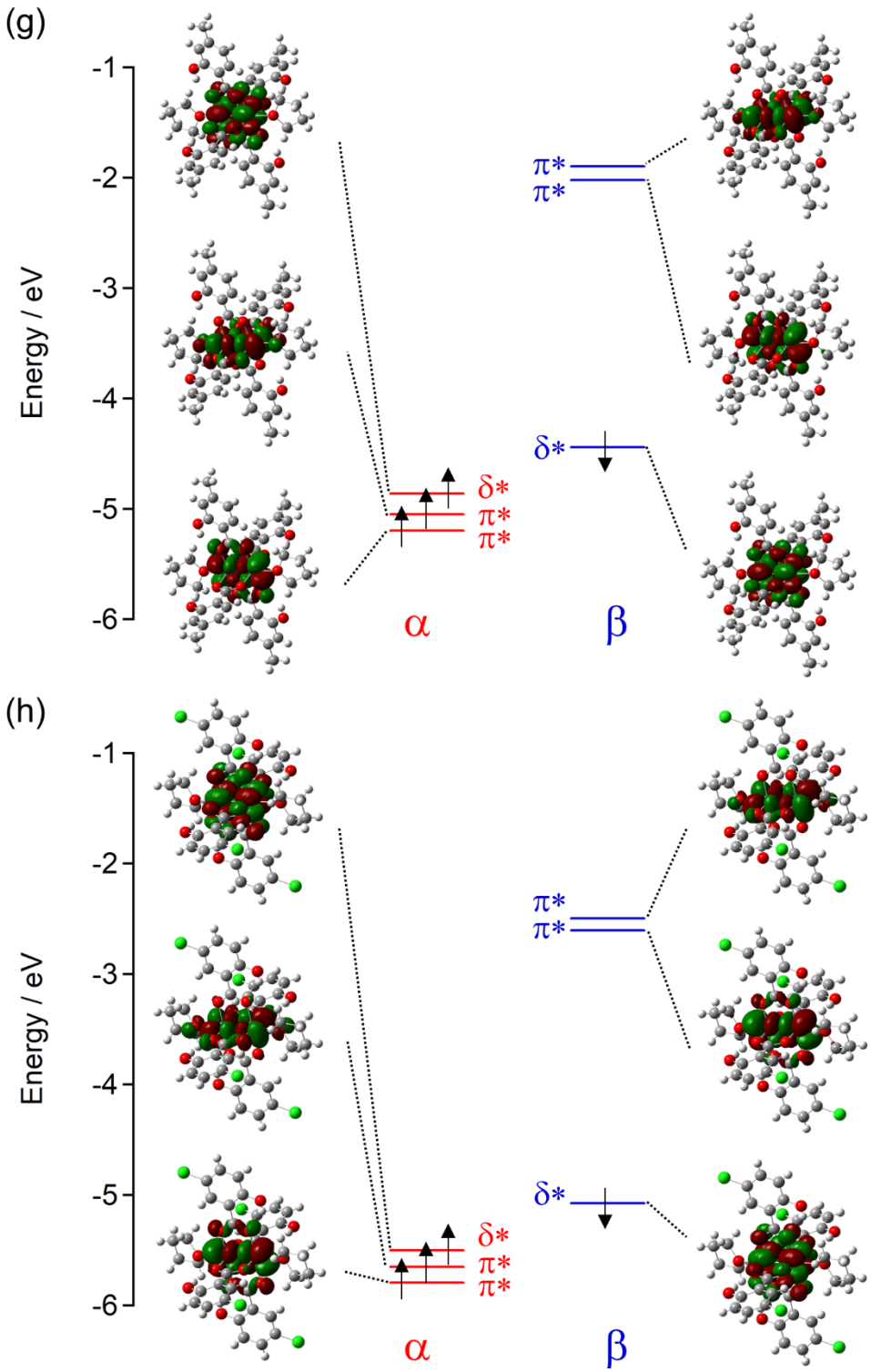

Fig. S6 (continued). Frontier orbitals associated with π* and δ* orbitals for **4Me2OH** (g) and **5Cl2OH** (h), and their energy levels (eV), where δ* for β electron corresponds to HOMO level.

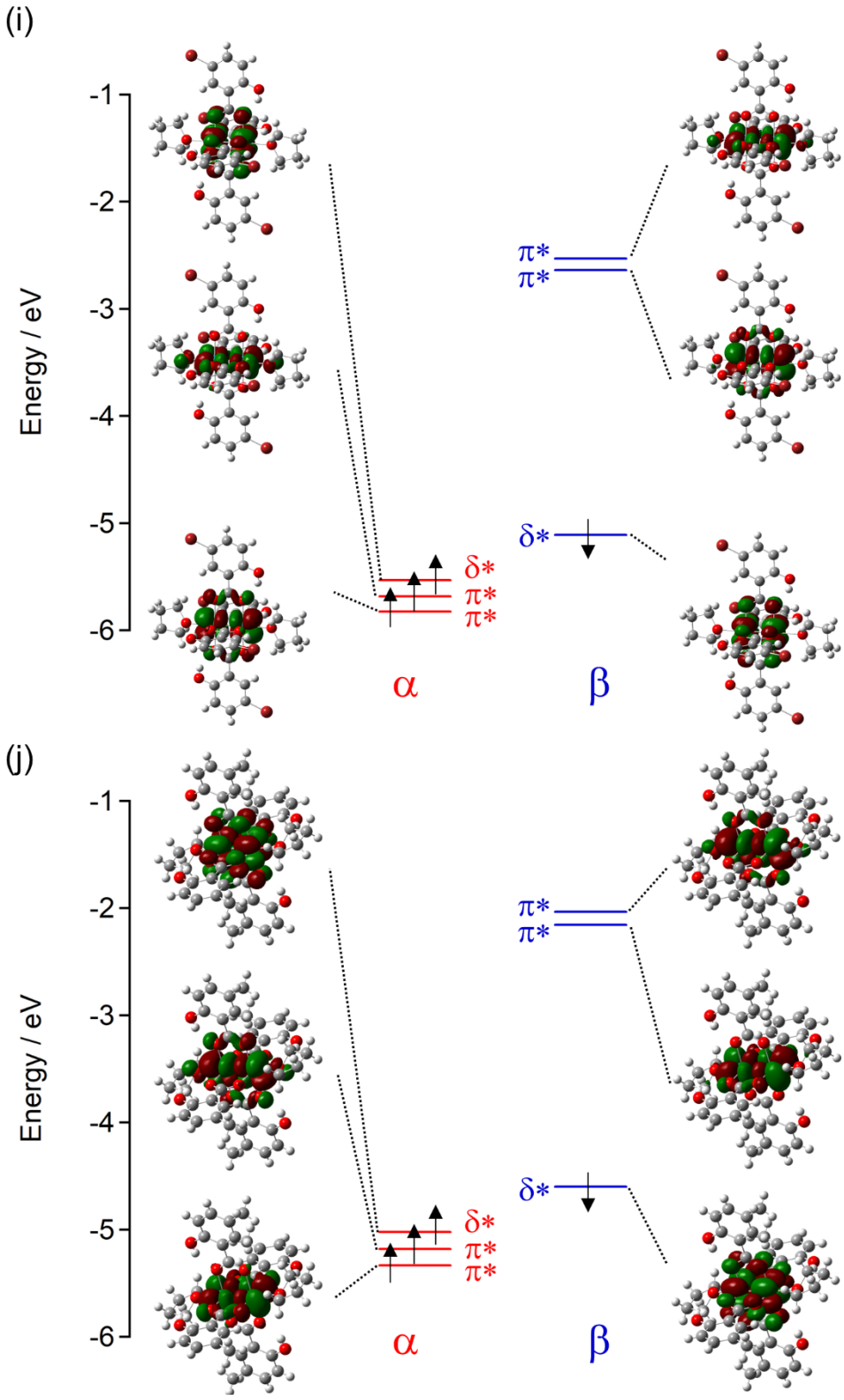

Fig. S6 (continued). Frontier orbitals associated with π* and δ* orbitals for **5Br2OH** (i) and **5Me2OH** (j), and their energy levels (eV), where δ* for β electron corresponds to HOMO level.

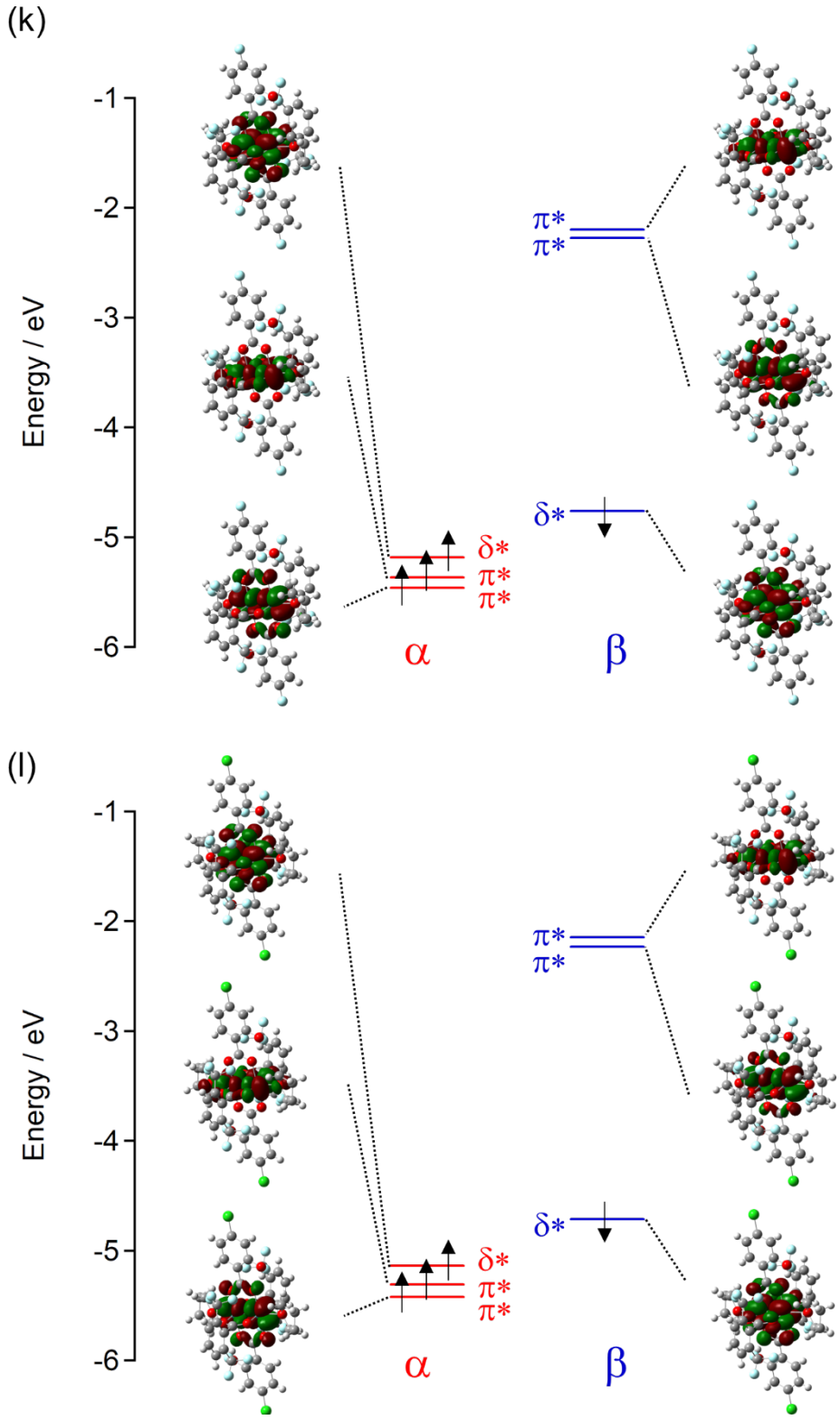

Fig. S6 (continued). Frontier orbitals associated with π* and δ* orbitals for **ht-4F2OH** (k) and **ht-4Cl2OH** (l), and their energy levels (eV), where δ* for β electron corresponds to HOMO level.

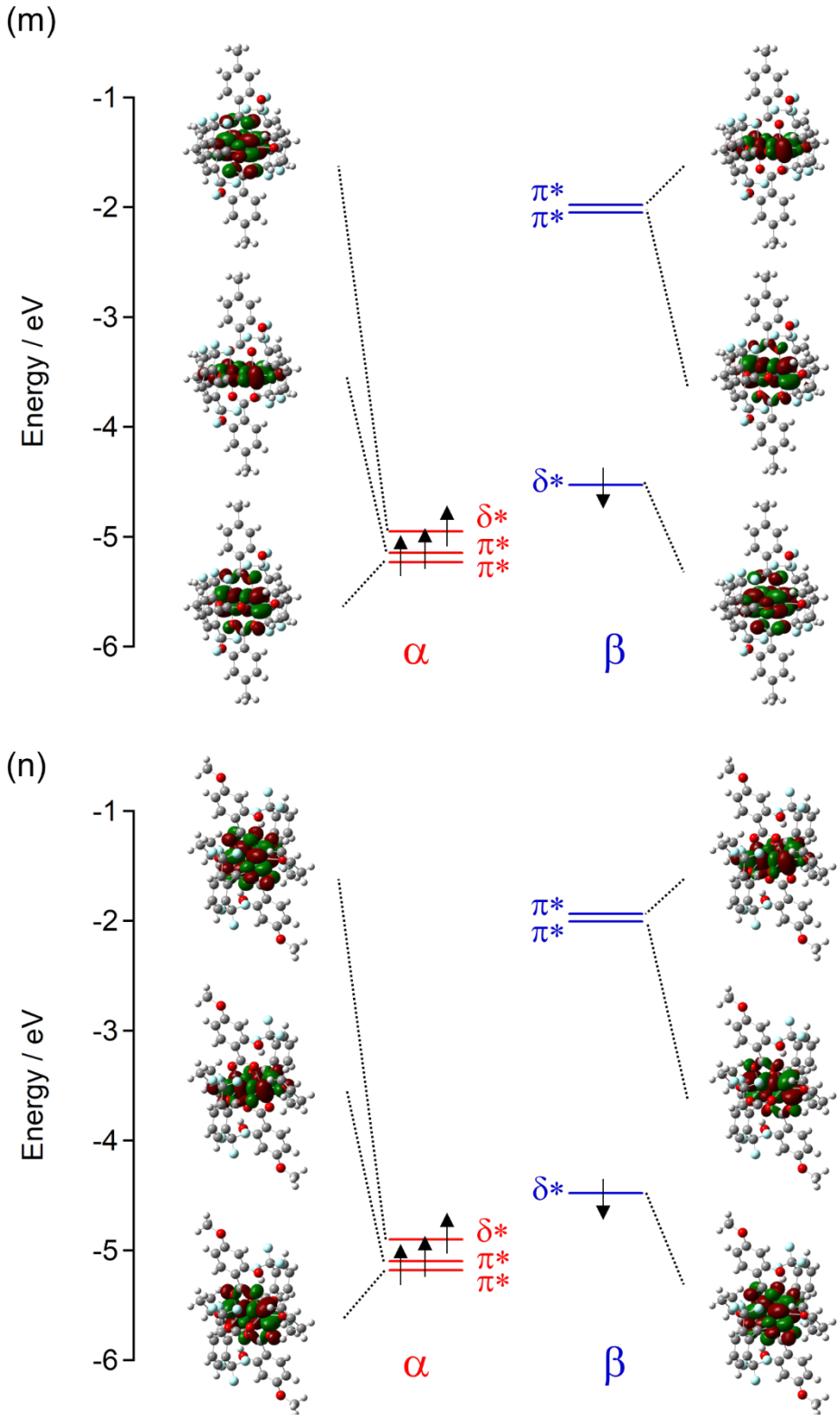

Fig. S6 (continued). Frontier orbitals associated with π* and δ* orbitals for **ht-4Me2OH** (m) and **ht-4OMe2OH** (n), and their energy levels (eV), where δ* for β electron corresponds to HOMO level.

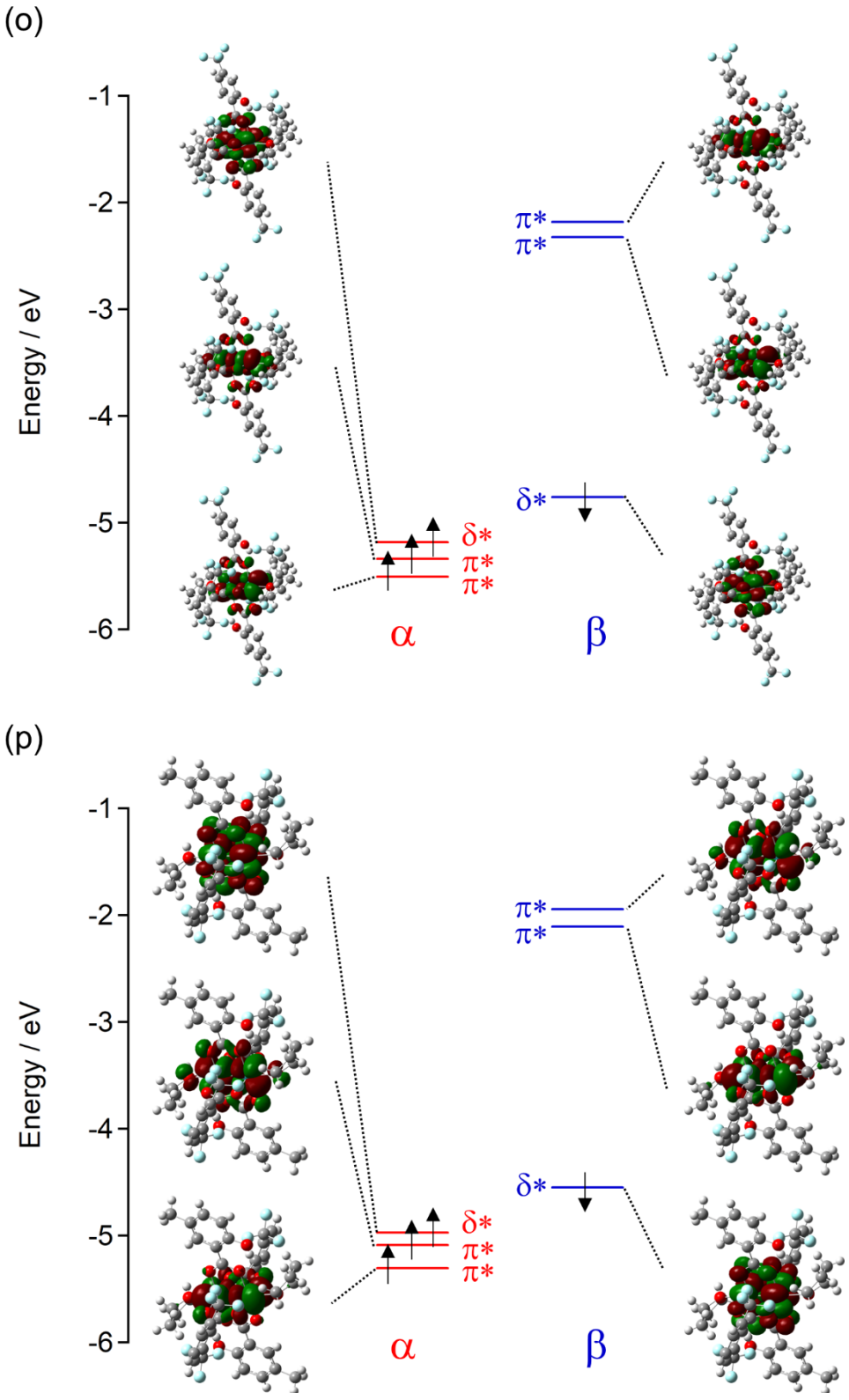

Fig. S6 (continued). Frontier orbitals associated with π* and δ* orbitals for **ht-4CF$_3$2OH** (o) and **ht-5Me2OH** (p), and their energy levels (eV), where δ* for β electron corresponds to HOMO level.

Table S6. Estimated energy levels (eV) of π*- and δ*-characteristic orbitals of the heteroleptic [$Ru_2^{II,II}$] complexes obtained by DFT calculation for the hypothetical structural models without intra-molecular hydrogen bond.

Electron character	**Orbital character**	**3F2OH**	**4F2OH**	**4Cl2OH**	**4Me2OH**
β	π*	−1.41472	−1.45771	−1.50561	−0.999203
	π*	−1.58098	−1.57418	−1.62071	−1.12519
	δ*	−3.99926	−4.00334	−4.03654	−3.52061
α	δ*	−4.42566	−4.42947	−4.46349	−3.94538
	π*	−4.54893	−4.60934	−4.65152	−4.14538
	π*	−4.74676	−4.74594	−4.78730	−4.28824

Electron character	**Orbital character**	**5Cl2OH**	**5Br2OH**	**5Me2OH**
β	π*	−1.53581	−1.57608	−1.00655
	π*	−1.64738	−1.68683	−1.1241
	δ*	−4.08688	−4.12579	−3.53857
α	δ*	−4.51464	−4.55328	−3.96497
	π*	−4.68526	−4.72635	−4.14756
	π*	−4.82132	−4.85968	−4.28498

Electron character	**Orbital character**	**ht-4F2OH**	**ht-4Cl2OH**	**ht-4Me2OH**	**ht-4OMe2OH**
β	π*	−1.72194	−1.67894	−1.51078	−1.47894
	π*	−1.75296	−1.72085	−1.53935	−1.50234
	δ*	−4.24416	−4.21042	−4.02429	−3.98402
α	δ*	−4.66703	−4.63356	−4.44634	−4.40471
	π*	−4.88989	−4.84472	−4.67927	−4.64907
	π*	−4.92309	−4.89234	−4.70812	−4.65560

Electron character	**Orbital character**	**ht-4$CF_3$2OH**	**ht-5Me2OH**
β	π*	−1.74044	−1.54996
	π*	−1.89609	−1.67405
	δ*	−4.31301	−4.07736
α	δ*	−4.73805	−4.49995
	π*	−4.89179	−4.60226
	π*	−5.07139	−4.87030

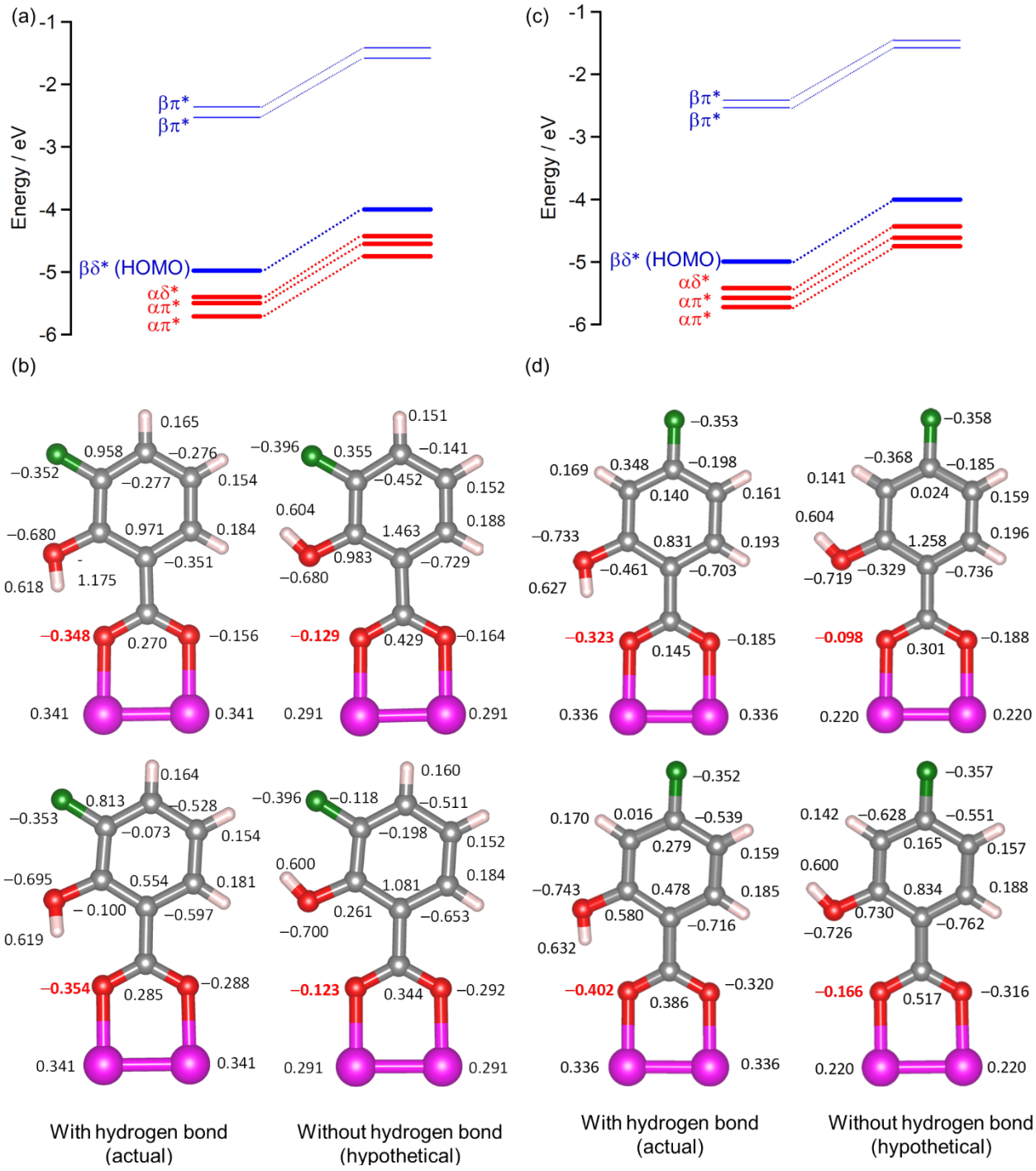

Fig. S7. Energy diagrams of frontier orbitals associated with π* and δ* orbitals for **3F2OH** (a) and **4F2OH** (c) obtained by DFT calculation for the structural models with (left) or without (right) intra-molecular hydrogen bond; a part of a structural model of **3F2OH** (b) and **4F2OH** (d) subjected to DFT calculation; actual (left) or hypothetical (right) crystal structure with or without intra-molecular hydrogen bond, respectively. The attached digits indicate the value of the Mulliken charge.[11] Another bridging benzoate ligands and THF molecules at the axial position are omitted for clarity.

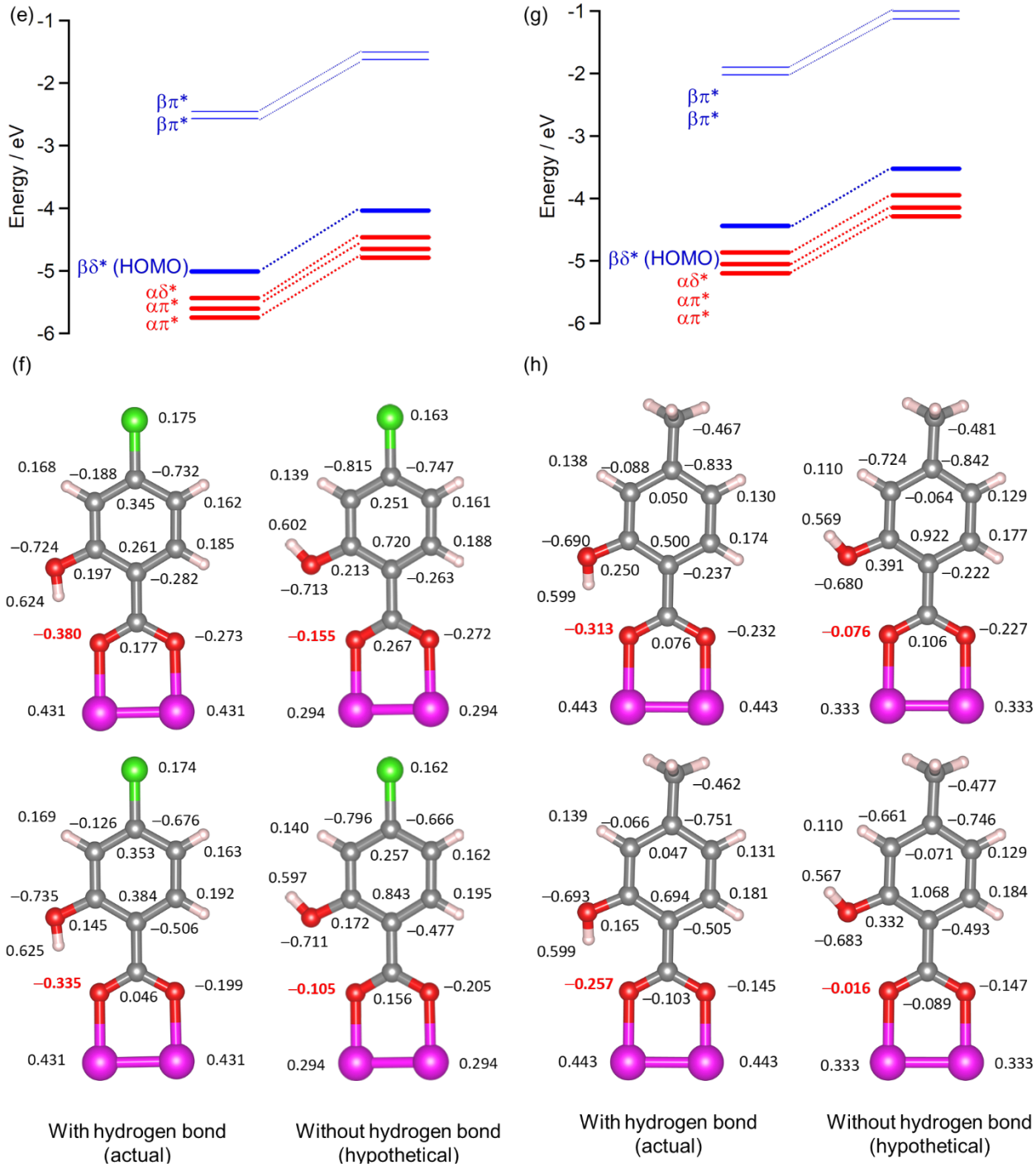

Fig. S7 (continued). Energy diagrams of frontier orbitals associated with π* and δ* orbitals for **4Cl2OH** (e) and **4Me2OH** (g) obtained by DFT calculation for the structural models with (left) or without (right) intra-molecular hydrogen bond; a part of a structural model of **4Cl2OH** (f) and **4Me2OH** (h) subjected to DFT calculation; actual (left) or hypothetical (right) crystal structure with or without intra-molecular hydrogen bond, respectively. The attached digits indicate the value of the Mulliken charge.[11] Those for hydrogen on sp3 carbon were omitted for clarity in Fig. S6h. Another bridging benzoate ligands and THF molecules at the axial position are omitted for clarity.

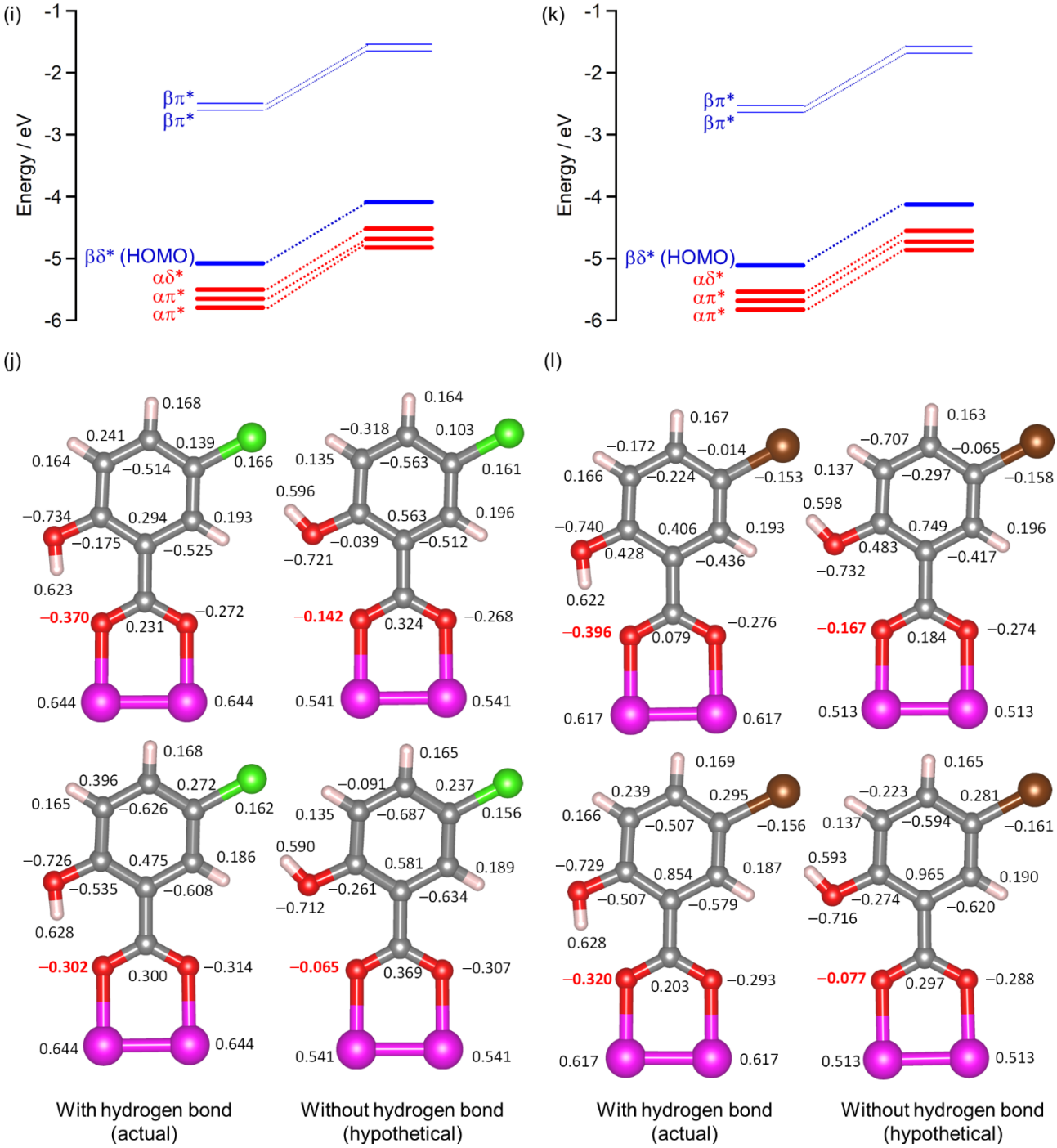

Fig. S7 (continued). Energy diagrams of frontier orbitals associated with π* and δ* orbitals for **5Cl2OH** (i) and **5Br2OH** (k) obtained by DFT calculation for the structural models with (left) or without (right) intra-molecular hydrogen bond; a part of a structural model of **5Cl2OH** (j) and **5Br2OH** (l) subjected to DFT calculation; actual (left) or hypothetical (right) crystal structure with or without intra-molecular hydrogen bond, respectively. The attached digits indicate the value of the Mulliken charge.[11] Another bridging benzoate ligands and THF molecules at the axial position are omitted for clarity.

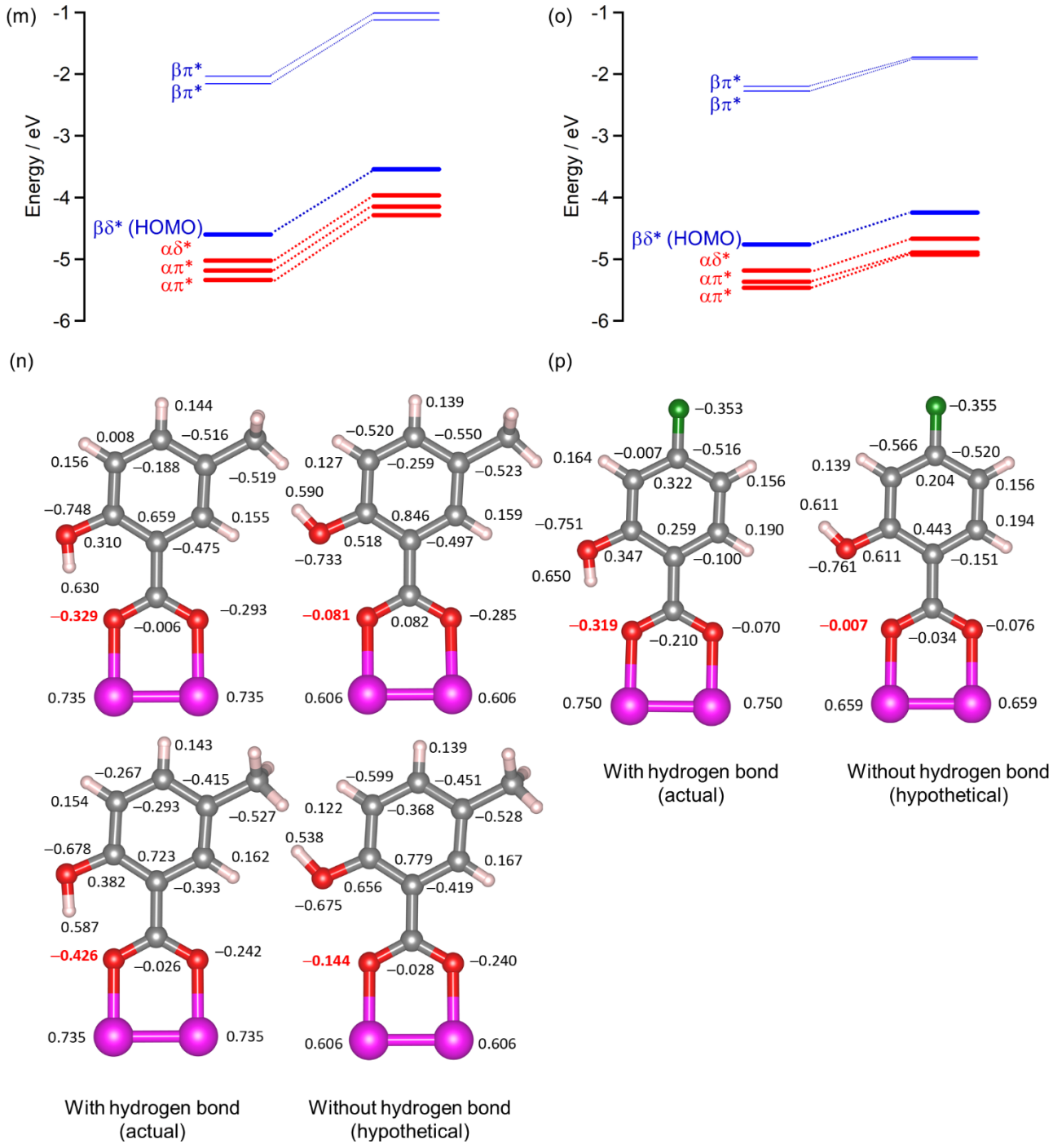

Fig. S7 (continued). Energy diagrams of frontier orbitals associated with π* and δ* orbitals for **5Me2OH** (m) and **ht-4F2OH** (o) obtained by DFT calculation for the structural models with (left) or without (right) intra-molecular hydrogen bond; a part of a structural model of **5Me2OH** (n) and **ht-4F2OH** (p) subjected to DFT calculation; actual (left) or hypothetical (right) crystal structure with or without intra-molecular hydrogen bond, respectively. The attached digits indicate the value of the Mulliken charge.[11] Those for hydrogen on sp3 carbon were omitted for clarity in Fig. S6n. Another bridging benzoate ligands and THF molecules at the axial position are omitted for clarity.

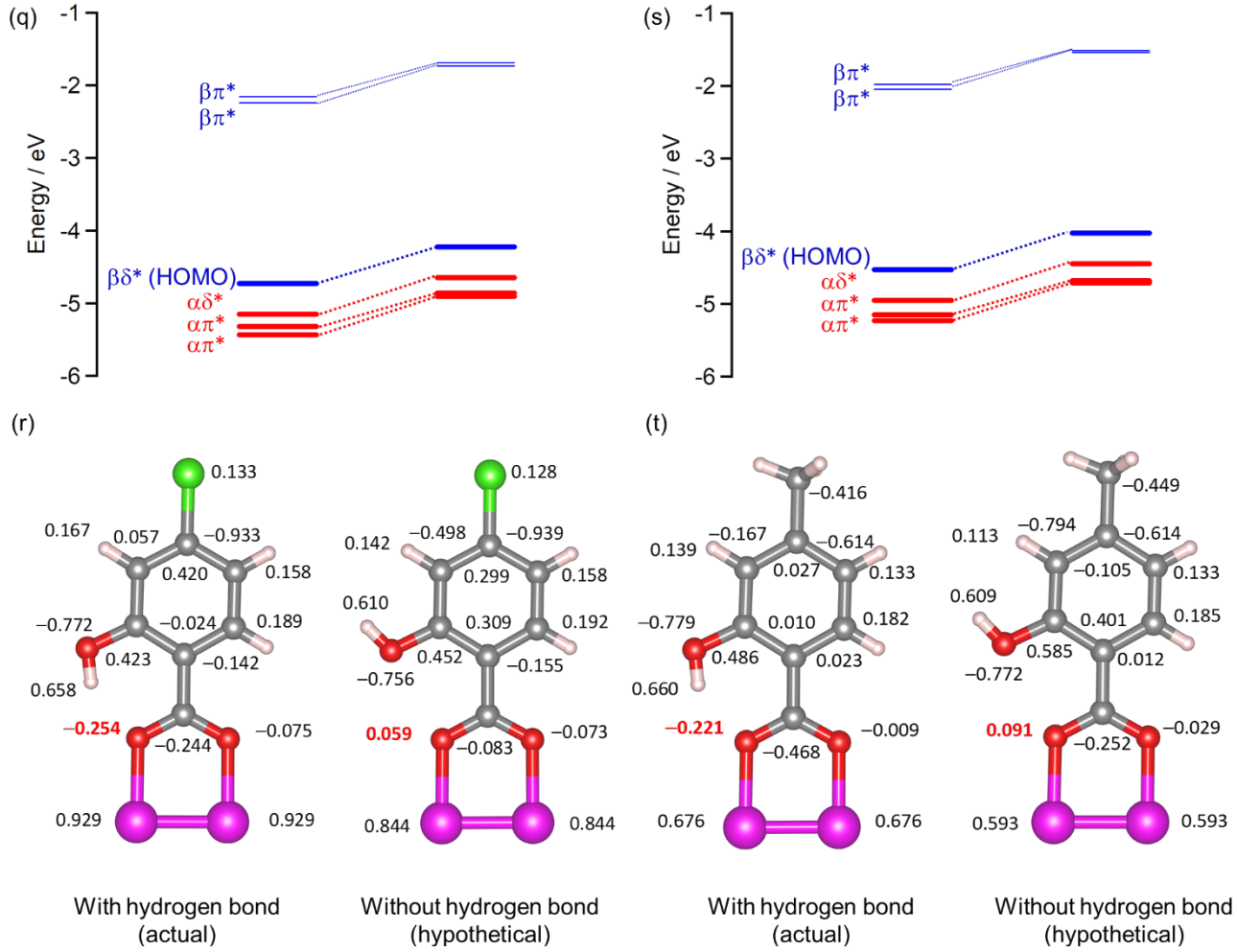

Fig. S7 (continued). Energy diagrams of frontier orbitals associated with π* and δ* orbitals for **ht-4Cl2OH** (q) and **ht-4Me2OH** (s) obtained by DFT calculation for the structural models with (left) or without (right) intra-molecular hydrogen bond; a part of a structural model of **ht-4Cl2OH** (r) and **ht-4Me2OH** (t) subjected to DFT calculation; actual (left) or hypothetical (right) crystal structure with or without intra-molecular hydrogen bond, respectively. The attached digits indicate the value of the Mulliken charge.[11] Those for hydrogen on sp3 carbon were omitted for clarity in Fig. S6t. Another bridging benzoate ligands and THF molecules at the axial position are omitted for clarity.

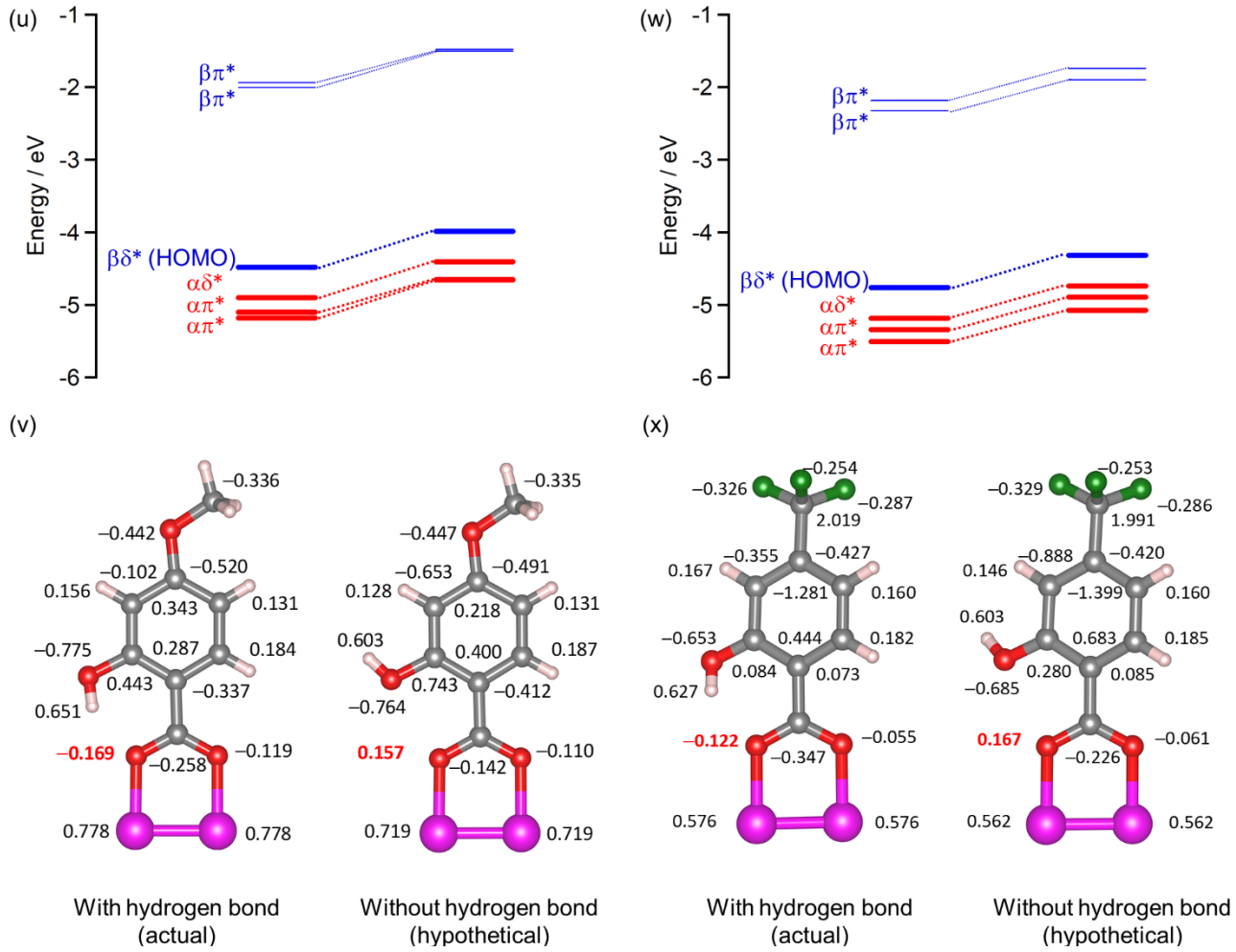

Fig. S7 (continued). Energy diagrams of frontier orbitals associated with π* and δ* orbitals for **ht-4OMe2OH** (u) and **ht-4CF$_3$2OH** (w) obtained by DFT calculation for the structural models with (left) or without (right) intra-molecular hydrogen bond; a part of a structural model of **ht-4OMe2OH** (v) and **ht-4CF$_3$2OH** (x) subjected to DFT calculation; actual (left) or hypothetical (right) crystal structure with or without intra-molecular hydrogen bond, respectively. The attached digits indicate the value of the Mulliken charge.[11] Those for hydrogen on sp3 carbon were omitted for clarity in Fig. S6v. Another bridging benzoate ligands and THF molecules at the axial position are omitted for clarity.

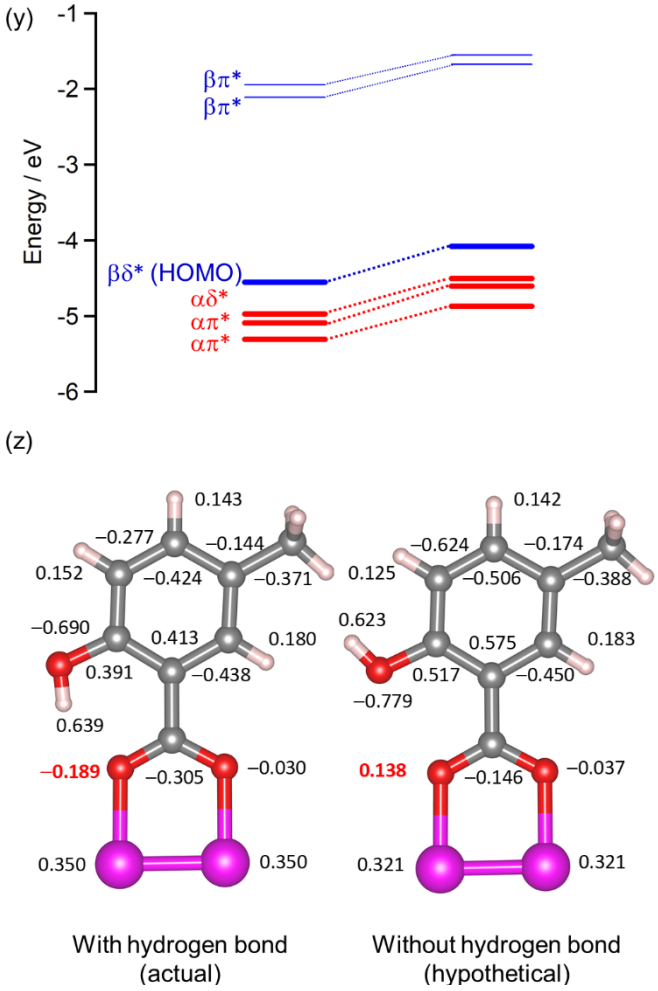

Fig. S7 (continued). Energy diagrams of frontier orbitals associated with π* and δ* orbitals for **ht-5Me2OH** (y) obtained by DFT calculation for the structural models with (left) or without (right) intra-molecular hydrogen bond; a part of a structural model of **ht-5Me2OH** (z) subjected to DFT calculation; actual (left) or hypothetical (right) crystal structure with or without intra-molecular hydrogen bond, respectively. The attached digits indicate the value of the Mulliken charge.[11] Those for hydrogen on sp3 carbon were omitted for clarity in Fig. S6z. Another bridging benzoate ligands and THF molecules at the axial position are omitted for clarity.

References for SI

1 W. Kosaka, M. Itoh and H. Miyasaka, *Dalton Trans.*, 2015, **44**, 8156−8168.
2 W. Kosaka, Y. Watanabe, K. H. Aliyah and H. Miyasaka, *Dalton Trans.*, 2022, **51**, 85−94.
3 W. Kosaka, T. Morita, T. Yokoyama, J. Zhang and H. Miyasaka, *Inorg. Chem.*, 2015, **54**, 1518−1527.
4 W. Kosaka, K. Yamagishi, A. Hori, H. Sato, R. Matsuda, S. Kitagawa, M. Takata and H. Miyasaka, *J. Am. Chem. Soc.*, 2013, **135**, 18469−18480.
5 H. Miyasaka, N. Motokawa, R. Atsuumi, H. Kamo, Y. Asai and M. Yamashita, *Dalton Trans.*, 2011, **40**, 673−682.
6 Y. Sekine, K. H. Aliyah, T. Shimada, J. Zhang, W. Kosaka and H. Miyasaka, *Chem. Lett.*, 2018, **47**, 693−696.
7 C. Itoh, H. Yoshino, T. Kitayama, W. Kosaka and H. Miyasaka, *Dalton Trans.*, 2024, **53**, 444−448.
8 J. Zhang, W. Kosaka, S. Kitagawa, M. Takata and H. Miyasaka, *Chem. −Eur. J.*, 2019, **25**, 3020−3031.
9 D. H. McDaniel and H. C. Brown, *J. Org. Chem.*, 1958, **23**, 420–427.
10 Y. Sekine, W. Kosaka, H. Kano, C. Dou, T. Yokoyama and H. Miyasaka, *Dalton Trans.*, 2016, **45**, 7427−7434.
11 R. S. Mulliken, *J. Chem. Phys.*, 1952, **23**, 1833−1840.